

# A Variable-Separation-based Domain Decomposition Method for Parametric Dynamical Systems\*

Yuming Ba<sup>†</sup>   Liang Chen<sup>‡§</sup>   Yaru Chen<sup>‡§</sup>   Qiuqi Li<sup>‡§</sup>

August 26, 2025

## Abstract

This paper proposes a model order reduction method for a class of parametric dynamical systems. Using a temporal Fourier integral transform, we reformulate these systems into complex-valued elliptic equations in the frequency domain, containing both the frequency variables and the parameters inherited from the original model. To reduce the computational cost of the frequency-variable elliptic equations, we extend the variable-separation-based domain decomposition method to the complex-valued context, resulting in an offline-online procedure for solving the parametric dynamical systems. In the offline stage, separate representations of the solutions for the interface problem and the subproblems are constructed. In the online stage for new parameter values, the solutions of the parametric dynamical systems can be directly derived by utilizing the separate representations and implementing the inverse Fourier transform. The proposed approach is capable of being highly efficient because the online stage is independent of the spatial discretization. Finally, we present three specific instances for parametric dynamical systems to demonstrate the effectiveness of the proposed method.

**Keywords:** parametric dynamical systems, model order reduction, domain decomposition, variable-separation method, Fourier transformation

**MSCcodes:** 35R60, 37M99, 65P99

## 1 Introduction

Parametric dynamical systems have been widely adopted in science and engineering to model complex real-world problems characterized by various uncertainties. These uncertainties may stem from multiple sources, including physical properties, geometric configurations, initial conditions, and boundary conditions. However, the numerical simulation of such parametric systems poses substantial computational challenges, especially in scenarios requiring repeated parameter evaluations for design optimization, control analysis, and uncertainty quantification. While traditional high-fidelity numerical methods, such as the finite element method (FEM), finite difference method, and finite volume method, can provide accurate solutions, they often entail extreme-scale computations with prohibitive computational costs.

Recognizing these limitations, researchers have developed numerous innovative numerical approaches over the past few decades to overcome the computational bottlenecks in simulating parametric dynamical systems. Among these, model order reduction (MOR) techniques, such

---

\*The research of this work was supported by the National Key R&D Program of China (No. 2021YFA001300), the National Natural Science Foundation of China (Nos. 12401567, 12271150, 12471405), the Hunan Provincial Natural Science Foundation of China (No. 2023JJ10001), and the Science and Technology Innovation Program of Hunan Province (No. 2022RC1190).

<sup>†</sup>School of Mathematics and Systems Science, Guangdong Polytechnic Normal University, Guangzhou 510665, China ([yumingba@gpnu.edu.cn](mailto:yumingba@gpnu.edu.cn)).

<sup>‡</sup>School of Mathematics, Hunan University, Changsha 410082, China ([chl@hnu.edu.cn](mailto:chl@hnu.edu.cn), [yrchen@hnu.edu.cn](mailto:yrchen@hnu.edu.cn), [qli28@hnu.edu.cn](mailto:qli28@hnu.edu.cn)).

<sup>§</sup>Hunan Provincial Key Laboratory of Intelligent Information Processing and Applied Mathematics, Changsha 410082, China.

as those discussed in [37, 1, 2, 29, 14, 16, 40], have emerged as a powerful tool. MOR constructs reduced-order models by approximating solutions in a low-dimensional subspace, significantly reducing computational costs. A prominent MOR approach is the reduced basis (RB) method (e.g., [17, 15, 18, 11, 23, 22]), which follows an offline-online computational strategy. In the offline phase, high-fidelity solutions for a carefully selected parameter set are precomputed and stored. The online phase then efficiently approximates solutions for new parameters via a linear combination of these precomputed solutions. In this method, the key challenge lies in constructing an optimal set of basis functions that accurately capture the essential features of the full order model.

An alternative approach for effectively reducing the computational cost of dynamical systems is the frequency-domain method, which relies on two key transformations: the Fourier transform [9, 10, 13, 26, 25] and the Laplace transform in the time dimension [27, 28]. The Fourier transform stands out as a significant discovery in mathematical sciences, playing a crucial role in modern scientific and technological advancements, which has been widely applied in the analysis of continuous-time systems, including signal and image processing, analog circuit analysis, and communication systems. The fundamental principle behind this approach is to convert time-dependent PDEs into frequency-dependent elliptic problems, which are stationary in time but parametrized by frequency. The time-domain solution is then reconstructed by applying an inverse Fourier transform to the frequency-domain solutions. A major advantage of this framework is its inherent suitability for parallel computation, i.e., each frequency can be solved independently as the resulting frequency-domain equations are decoupled. For the frequency-domain equations that require numerous solutions, MOR techniques have demonstrated the effectiveness [7, 21, 1]. A low-order Galerkin proper orthogonal decomposition basis is employed to approximate solutions for frequency-domain equations in [39]. It adopts the Gaussian quadrature rule based on Legendre-Gauss-Lobatto (LGL) points to enable a precise numerical integration of the inverse Fourier transformation.

In this paper, we focus on the frequency-domain method based on Fourier transform. It reformulates parametric dynamical systems into frequency-variable parametric elliptic equations (which are time-independent). Although the Fourier transform has converted the time-domain problem into a frequency-domain problem (eliminating the time variable), the transformed equations remain dependent on spatial discretization. In addition, repeatedly solving of the frequency-variable parametric elliptic equations is necessary to approximate the solutions of the original problems. The computational cost is expensive when the inverse Fourier transform contains a large number of frequencies. Therefore, the MOR is necessary for the frequency-variable parametric elliptic equations. As one of the MOR methods, the variable-separation (VS) method [30] has been verified to be able to provide accurate and efficient approximate solutions to stochastic PDEs. Then, [24] has extended the VS to stochastic saddle point problems. For nonlinear PDEs with random inputs, the VS method also has illustrated the effectiveness in [31]. Moreover, it has been used to the non-overlapping domain decomposition method (DDM) for stochastic PDEs in [5], and to the parametric dynamical systems in [6]. To improve the computational efficiency of the frequency-variable parametric elliptic equations, we consider the variable-separation-based domain decomposition (DD-VS) method [5] instead of the VS method, as the DD-VS method enables efficient online computations and is well-suited for handling heterogeneous problems.

The DD-VS method is based on the non-overlapping DDM [3, 36, 41, 19, 32, 8], which establishes a relationship between the input parameters and the interface problem of the parametric PDEs. It features an offline-online computational decomposition. During the offline phase, the Schur complement method [33, 20, 38] is applied to construct the interface problem. However, this problem is dense and requires the inversion of random matrices. To enhance computational efficiency, the extended VS method is employed to transform the interface problem into a reduced algebraic system. This transformation utilizes low-rank representations of the global Schur complement matrices and right-hand side vectors. While the reduced model significantly reduces computational costs relative to the original interface problem, it retains dependencies on the full model's discrete degrees of freedom and thus cannot be classified as truly small-scale. To further streamline computation, the VS method is used once again to create a surrogate

model for the reconstructed interface problem. The online phase then efficiently evaluates new samples using this surrogate model, enabling rapid recovery of interface solutions. Additionally, the VS method can also be used to obtain an efficient surrogate model for the subproblem. Notably, the online computation is highly efficient due to the reduced-order representation of the interface solution, and its computational cost is entirely independent of spatial discretization. Overall, the DD-VS method provides efficient and reliable approximations for parametric PDEs, enabling the construction of low-rank approximate solutions to the frequency-variable elliptic equations.

Actually, although the solutions of frequency-variable elliptic equations are complex-valued, the DD-VS method can still be applied to these equations, effectively reducing computational costs, especially for heterogeneous problems. In this context, since all elements within both the interface problem and the subproblems are complex-valued, an extension of the VS method to complex-valued situations is required. To achieve this, we decompose the complex-valued problem into its real and imaginary components, thereby formulating a system for these parts. By following the procedures of the VS method for real-valued elliptic equations, we are able to derive separate affine surrogate models for the real and imaginary components. This enables the DD-VS method to efficiently compute both the interface problem and subproblems during the online phase, while maintaining its effectiveness for complex-valued frequency-dependent elliptic equations.

In this paper, by combining the complex-valued DD-VS method with Fourier transformation, we develop a reduced order method for time-dependent problems, which can be regarded as an extension of the DD-VS method. The process begins with applying the Fourier transform to reformulate the time-dependent problems into frequency-variable elliptic equations. Subsequently, leveraging the existing DD-VS method for complex-valued scenarios, we construct efficient surrogate models for both the interface problem and subproblems during the offline stage. The resulting online computation exhibits remarkable efficiency because, for new parameters, the cost only depends on computing the parametric coefficients in the surrogate model and performing the inverse Fourier transform. Crucially, the online phase remains independent of the spatial discretization of the original problem and requires no temporal recomputation, thereby ensuring remarkable efficiency in solving time-dependent problems.

This paper is organized as follows. Section 2 provides the necessary notation and preliminaries, introduces the Fourier transform for the time variable and the VS method for parametric complex-valued systems. It also provides a brief overview of the domain decomposition method for deterministic complex-valued PDEs. In Section 4, we present the DD-VS method proposed in this paper, detailing its key steps and procedures. In Section 5, three numerical examples are presented to demonstrate the performance and computational advantages of the proposed method. Finally, we draw conclusions and offer some final remarks on the method and its potential applications.

## 2 Preliminaries

Let  $\Omega$  be the set representing the parameter domain. We use  $\boldsymbol{\xi} \in \Omega$  to represent a vector of parametric inputs. Given an open and bounded spatial domain  $D \subset \mathbb{R}^d$  with Lipschitz continuous boundary  $\partial D$ , we consider the parametric dynamical system

$$\begin{cases} \frac{\partial u}{\partial t}(\mathbf{x}, t; \boldsymbol{\xi}) = \mathcal{F}(u(\mathbf{x}, t; \boldsymbol{\xi}); \boldsymbol{\xi}) & \forall \mathbf{x} \in D, t \in [0, T], \boldsymbol{\xi} \in \Omega, \\ u(\mathbf{x}, 0; \boldsymbol{\xi}) = u_0(\mathbf{x}; \boldsymbol{\xi}) & \forall \mathbf{x} \in D, \boldsymbol{\xi} \in \Omega, \\ \mathcal{B}(u(\mathbf{x}, t; \boldsymbol{\xi})) = g(\mathbf{x}, t; \boldsymbol{\xi}) & \forall \mathbf{x} \in \partial D, t \in [0, T], \boldsymbol{\xi} \in \Omega, \end{cases}$$

where  $u(\cdot, t; \boldsymbol{\xi})$  is desired the solution to this system,  $g(\cdot, t; \boldsymbol{\xi})$  is the boundary term, and  $u_0(\cdot; \boldsymbol{\xi})$  is the initial condition. The interval  $[0, T]$  is regarded as the temporal domain. To simplify the presentation, we illustrate our methodology using the following parametric parabolic partial

differential equation as a representative example

$$\begin{cases} \frac{\partial u}{\partial t}(\mathbf{x}, t; \boldsymbol{\xi}) - \nabla \cdot (c(\mathbf{x}; \boldsymbol{\xi}) \nabla u(\mathbf{x}, t; \boldsymbol{\xi})) = f(\mathbf{x}, t; \boldsymbol{\xi}) & \forall \mathbf{x} \in D, t \in [0, T], \boldsymbol{\xi} \in \Omega, \\ u(\mathbf{x}, 0; \boldsymbol{\xi}) = u_0(\mathbf{x}; \boldsymbol{\xi}) & \forall \mathbf{x} \in D, \boldsymbol{\xi} \in \Omega, \\ u(\mathbf{x}, t; \boldsymbol{\xi}) = g(\mathbf{x}, t; \boldsymbol{\xi}) & \forall \mathbf{x} \in \partial D, t \in [0, T], \boldsymbol{\xi} \in \Omega, \end{cases} \quad (2.1)$$

where  $c(\mathbf{x}; \boldsymbol{\xi})$  denotes a diffusion coefficient that depends on the spatial variable  $\mathbf{x}$  and the parameter  $\boldsymbol{\xi}$ .

Define  $\mathcal{V} := L^2(D; \mathbb{C}) = \{\hat{u}(\mathbf{x}) \mid \int_D |\hat{u}(\mathbf{x})|^2 dx < +\infty\}$ , where  $|\hat{u}(\mathbf{x})|$  denotes the modulus of the complex-valued function  $\hat{u}(\mathbf{x})$ . Moreover, the inner product of  $\mathcal{V}$  and the associated norm are defined by

$$\langle \hat{u}(\mathbf{x}), \hat{v}(\mathbf{x}) \rangle := \int_D \hat{u}(\mathbf{x}) \overline{\hat{v}(\mathbf{x})} dx \quad \text{and} \quad \|\hat{u}(\mathbf{x})\| := \sqrt{\langle \hat{u}(\mathbf{x}), \hat{u}(\mathbf{x}) \rangle}.$$

## 2.1 The frequency-domain method

To tackle the dynamical system (2.1), we apply the Fourier transformation to get the following set of complex-valued elliptic equations depending on the frequency  $\omega$

$$\begin{cases} i\omega \hat{u}(\mathbf{x}, \omega; \boldsymbol{\xi}) - \nabla \cdot (c(\mathbf{x}; \boldsymbol{\xi}) \nabla \hat{u}(\mathbf{x}, \omega; \boldsymbol{\xi})) = \hat{f}(\mathbf{x}, \omega; \boldsymbol{\xi}) & \forall \mathbf{x} \in D, \boldsymbol{\xi} \in \Omega, \\ \hat{u}(\mathbf{x}, \omega; \boldsymbol{\xi}) = \hat{g}(\mathbf{x}, \omega; \boldsymbol{\xi}) & \forall \mathbf{x} \in \partial D, \boldsymbol{\xi} \in \Omega \end{cases} \quad (2.2)$$

where  $i = \sqrt{-1}$  is the imaginary unit. The Fourier transform  $\hat{u}(\mathbf{x}, \omega; \boldsymbol{\xi})$  of a function  $u(\mathbf{x}, t; \boldsymbol{\xi})$  in time and the Fourier inversion are given by

$$\begin{cases} \hat{u}(\mathbf{x}, \omega; \boldsymbol{\xi}) := \int_{-\infty}^{\infty} u(\mathbf{x}, t; \boldsymbol{\xi}) \exp(-i\omega t) dt, \\ u(\mathbf{x}, t; \boldsymbol{\xi}) := \frac{1}{2\pi} \int_{-\infty}^{\infty} \hat{u}(\mathbf{x}, \omega; \boldsymbol{\xi}) \exp(i\omega t) d\omega. \end{cases}$$

For the Fourier transformation, the function  $u$  is zero-extended outside the interval  $[0, T]$  (i.e., for  $t < 0$  and  $t > T$ ) with the functions  $f$  and  $g$  being treated identically to derive equation (2.2).

The weak formulation of (2.2) reads as follows: for all  $\omega \in \mathbb{R}$  and  $\boldsymbol{\xi} \in \Omega$ , find  $\hat{u}(\cdot, \omega; \boldsymbol{\xi}) \in \mathcal{V}$  such that

$$\langle \hat{u} \hat{u}(\cdot, \omega; \boldsymbol{\xi}) - \nabla \cdot (c(\cdot; \boldsymbol{\xi}) \nabla \hat{u}(\cdot, \omega; \boldsymbol{\xi})), \hat{v} \rangle = \langle \hat{f}(\cdot, \omega; \boldsymbol{\xi}), \hat{v} \rangle \quad \forall \hat{v} \in \mathcal{V}. \quad (2.3)$$

Consider the finite element approximation of problem (2.3) in an  $n$ -dimensional subspace  $\mathcal{V}_h \subset \mathcal{V}$ . Let  $\{\psi_j\}_{j=1}^n$  be the set of basis functions of the space  $\mathcal{V}_h$ , the solution  $\hat{u}(\mathbf{x}, \omega; \boldsymbol{\xi})$  can be approximated as

$$\hat{u}(\mathbf{x}, \omega; \boldsymbol{\xi}) \approx \hat{u}_h(\mathbf{x}, \omega; \boldsymbol{\xi}) := \sum_{j=1}^n \hat{u}_j(\omega; \boldsymbol{\xi}) \psi_j(\mathbf{x}),$$

where each  $\hat{u}_j(\omega; \boldsymbol{\xi}) := \hat{u}_j^{Re}(\omega; \boldsymbol{\xi}) + i\hat{u}_j^{Im}(\omega; \boldsymbol{\xi})$ ,  $j = 1, \dots, n$ , is a complex-valued function. For the approximation of the Fourier inversion, we apply the Gaussian quadrature rule based on the LGL-points with an appropriate interval  $[0, \omega^*]$  for a sufficiently large  $\omega^*$ , where  $\hat{u}(\cdot, \omega; \cdot)$  is negligible for  $|\omega| > \omega^*$ . Let  $\{\omega_j\}_{j=1}^{N_\omega}$  be the set of LGL-points on the interval  $[0, \omega^*]$ . Then, the time-variable approximate  $u(\mathbf{x}, t; \boldsymbol{\xi})$  to problem (2.1) is obtained via

$$u(\mathbf{x}, t; \boldsymbol{\xi}) = \frac{1}{\pi} \Re \left( \sum_{j=1}^{N_\omega} \hat{u}_h(\mathbf{x}, \omega_j; \boldsymbol{\xi}) \exp(i\omega_j t) w_j \right), \quad (2.4)$$

where  $w_j$  is the Gaussian quadrature weight of the LGL-points  $\omega_j$ .

Note that, for different values of  $\omega$  and  $\boldsymbol{\xi}$ , one has to solve (2.3) repetitively to obtain the solution  $\hat{u}_h(\mathbf{x}, \omega; \boldsymbol{\xi})$ . This process requires a large amount of computation when dealing with a large number of parameters  $\omega$  and  $\boldsymbol{\xi}$ , especially for more complex problems. To reduce the computational cost, the frequency variable  $\omega$  will be treated as a one-dimensional parameter in this paper. We aim to construct the reduced order model of  $\hat{u}_h(\mathbf{x}, \omega; \boldsymbol{\xi})$ . With this reduced order model, Eq. (2.4) can be computed in a computationally economical fashion, and the implementation details will be elaborated in the following sections.

### 3 VS method and domain decomposition method

In this section, we will present in detail the VS method and the domain decomposition method for the complex-valued problem (2.3), where the VS method will be utilized in the next section to construct surrogate models for domain-decomposed problems.

#### 3.1 VS method for complex-valued problems

As described above, the goal of this paper is to build a reduced-order model when  $\omega$  is also considered as a parameter. In this subsection, the VS method will be extended to derive a separate representation of the solutions  $\hat{u}(\mathbf{x}, \omega; \boldsymbol{\xi})$  for the complex-valued elliptic problem (2.3). For convenience, define  $\boldsymbol{\mu} := (\omega, \boldsymbol{\xi})$  and  $\tilde{\Omega} := \mathbb{R} \times \Omega$ . Then the equality (2.3) can be rewritten as

$$a(\hat{u}, \hat{v}; \boldsymbol{\mu}) = b(\hat{v}; \boldsymbol{\mu}), \quad (3.1)$$

where  $a(\cdot, \cdot; \boldsymbol{\mu})$  and  $b(\cdot; \boldsymbol{\mu})$  are complex-valued bilinear and linear forms on  $\mathcal{V}$ , respectively. Assume that  $a(\cdot, \cdot; \boldsymbol{\mu})$  and  $b(\cdot; \boldsymbol{\mu})$  are affine with respect to  $\boldsymbol{\mu}$ , i.e.,

$$\begin{cases} a(\hat{u}, \hat{v}; \boldsymbol{\mu}) = \sum_{j=1}^{m_a} \alpha_j(\boldsymbol{\mu}) a_j(\hat{u}, \hat{v}) + i\gamma(\boldsymbol{\mu}) m(\hat{u}, \hat{v}) \quad \forall \hat{u}, \hat{v} \in \mathcal{V}, \forall \boldsymbol{\mu} \in \tilde{\Omega}, \\ b(\hat{v}; \boldsymbol{\mu}) = \sum_{j=1}^{m_b} \left( \beta_j^{Re}(\boldsymbol{\mu}) b_j^{Re}(\hat{v}) + i\beta_j^{Im}(\boldsymbol{\mu}) b_j^{Im}(\hat{v}) \right) \quad \forall \hat{v} \in \mathcal{V}, \forall \boldsymbol{\mu} \in \tilde{\Omega}, \end{cases} \quad (3.2)$$

where  $\gamma(\boldsymbol{\mu}) = \omega$ ,  $m(\hat{u}, \hat{v}) = \langle \hat{u}, \hat{v} \rangle$ ,  $\alpha_j(\boldsymbol{\mu}) : \tilde{\Omega} \rightarrow R$  is  $\boldsymbol{\mu}$ -dependent function and  $a_j : \mathcal{V} \times \mathcal{V} \rightarrow R$  is a bilinear form independent of  $\boldsymbol{\mu}$ , for each  $j = 1, \dots, m_a$ ,  $\beta_j^{Re}(\boldsymbol{\mu}) : \tilde{\Omega} \rightarrow R$  and  $\beta_j^{Im}(\boldsymbol{\mu}) : \tilde{\Omega} \rightarrow R$  are  $\boldsymbol{\mu}$ -dependent functions,  $b_j^{Re} : \mathcal{V} \rightarrow R$  and  $b_j^{Im} : \mathcal{V} \rightarrow R$  are linear forms independent of  $\boldsymbol{\mu}$ , for  $j = 1, \dots, m_b$ . Our analysis shows that affine decompositions play a crucial role in enabling the offline-online decomposition.

When (3.2) holds, the matrix form of Eq. (2.3) in a finite element space  $\mathcal{V}_h$  is given by

$$\left( \sum_{j=1}^{m_a} \alpha_j(\boldsymbol{\mu}) A_j + i\gamma(\boldsymbol{\mu}) M \right) \hat{\mathbf{u}}(\boldsymbol{\mu}) = \sum_{j=1}^{m_b} (\beta_j^{Re}(\boldsymbol{\mu}) F_j^{Re} + i\beta_j^{Im}(\boldsymbol{\mu}) F_j^{Im}), \quad (3.3)$$

where  $\hat{\mathbf{u}}(\boldsymbol{\mu}) = \hat{\mathbf{u}}^{Re}(\boldsymbol{\mu}) + i\hat{\mathbf{u}}^{Im}(\boldsymbol{\mu})$ , and

$$(A_j)_{kl} = a_j(\psi_k, \psi_l), \quad M_{kl} = \langle \psi_k, \psi_l \rangle, \quad (\hat{\mathbf{u}}^{Re}(\boldsymbol{\mu}))_k = \hat{u}_k^{Re}(\boldsymbol{\mu}), \quad (\hat{\mathbf{u}}^{Im}(\boldsymbol{\mu}))_k = \hat{u}_k^{Im}(\boldsymbol{\mu}), \\ (F_j^{Re})_k = b_j^{Re}(\psi_k), \quad (F_j^{Im})_k = b_j^{Im}(\psi_k), \quad 1 \leq k, l \leq n.$$

Now, we introduce the VS method for the problem (3.3) to obtain a separate approximation of the solution, i.e.,

$$\hat{\mathbf{u}}(\boldsymbol{\mu}) \approx \hat{\mathbf{u}}_N(\boldsymbol{\mu}) := \sum_{j=1}^N (\zeta_j^{Re}(\boldsymbol{\mu}) \mathbf{c}_j^{Re} + i\zeta_j^{Im}(\boldsymbol{\mu}) \mathbf{c}_j^{Im}), \quad (3.4)$$

where  $\zeta_j^{Re}(\boldsymbol{\mu})$  and  $\zeta_j^{Im}(\boldsymbol{\mu})$  are real-valued parametric functions dependent on  $\boldsymbol{\mu}$ ,  $\mathbf{c}_j^{Re}$  and  $\mathbf{c}_j^{Im}$  are real-valued vectors independent of  $\boldsymbol{\mu}$ , and  $N (\ll n)$  is the number of the separate terms. We define the residual of the VS method by

$$\mathbf{e}(\boldsymbol{\mu}) := \mathbf{e}^{Re}(\boldsymbol{\mu}) + i\mathbf{e}^{Im}(\boldsymbol{\mu}) = \hat{\mathbf{u}}(\boldsymbol{\mu}) - \hat{\mathbf{u}}_{k-1}(\boldsymbol{\mu}), \quad (3.5)$$

where  $\hat{\mathbf{u}}_{k-1}(\boldsymbol{\mu}) \equiv 0$  at  $k = 1$ . Substituting Eq.(3.5) into Eq. (3.3), we obtain

$$-\gamma(\boldsymbol{\mu}) M \mathbf{e}^{Im}(\boldsymbol{\mu}) + \sum_{j=1}^{m_a} \alpha_j(\boldsymbol{\mu}) A_j \mathbf{e}^{Re}(\boldsymbol{\mu}) = \mathbf{r}_k^{Re}(\boldsymbol{\mu}), \quad (3.6)$$

$$\gamma(\boldsymbol{\mu}) M \mathbf{e}^{Re}(\boldsymbol{\mu}) + \sum_{j=1}^{m_a} \alpha_j(\boldsymbol{\mu}) A_j \mathbf{e}^{Im}(\boldsymbol{\mu}) = \mathbf{r}_k^{Im}(\boldsymbol{\mu}), \quad (3.7)$$

where

$$\mathbf{r}_k^{Re}(\boldsymbol{\mu}) := \begin{cases} \sum_{j=1}^{m_b} \beta_j^{Re}(\boldsymbol{\mu}) F_j^{Re}, & k = 1, \\ \sum_{j=1}^{m_b} \beta_j^{Re}(\boldsymbol{\mu}) F_j^{Re} + \gamma(\boldsymbol{\mu}) M \hat{\mathbf{u}}_{k-1}^{Im}(\boldsymbol{\mu}) - \sum_{j=1}^{m_a} \alpha_j(\boldsymbol{\mu}) A_j \hat{\mathbf{u}}_{k-1}^{Re}(\boldsymbol{\mu}), & k \geq 2, \end{cases} \quad (3.8)$$

and

$$\mathbf{r}_k^{Im}(\boldsymbol{\mu}) := \begin{cases} \sum_{j=1}^{m_b} \beta_j^{Im}(\boldsymbol{\mu}) F_j^{Im}, & k = 1, \\ \sum_{j=1}^{m_b} \beta_j^{Im}(\boldsymbol{\mu}) F_j^{Im} - \gamma(\boldsymbol{\mu}) M \hat{\mathbf{u}}_{k-1}^{Re}(\boldsymbol{\mu}) - \sum_{j=1}^{m_a} \alpha_j(\boldsymbol{\mu}) A_j \hat{\mathbf{u}}_{k-1}^{Im}(\boldsymbol{\mu}), & k \geq 2. \end{cases} \quad (3.9)$$

At the  $k$ -th step, we choose  $\boldsymbol{\mu}_k$  as follows

$$\boldsymbol{\mu}_k := \begin{cases} \text{chosen randomly in } \Xi, & k = 1, \\ \operatorname{argmax}_{\boldsymbol{\mu} \in \Xi} |\mathbf{r}_k(\boldsymbol{\mu})|, & k \geq 2, \end{cases}$$

where  $\Xi$  is a collection of a finite number of samples in  $\tilde{\Omega}$ , and  $|\mathbf{r}_k(\boldsymbol{\mu})|$  is the modulus of  $\mathbf{r}_k(\boldsymbol{\mu}) := \mathbf{r}_k^{Re}(\boldsymbol{\mu}) + i\mathbf{r}_k^{Im}(\boldsymbol{\mu})$ . By solving equations (3.6-3.7) with  $\boldsymbol{\mu} = \boldsymbol{\mu}_k$ , we can derive  $\mathbf{c}_k^{Re} := \mathbf{e}^{Re}(\boldsymbol{\mu}_k)$  and  $\mathbf{c}_k^{Im} := \mathbf{e}^{Im}(\boldsymbol{\mu}_k)$  in (3.4), respectively.

Let  $\tilde{\mathbf{e}}^{Re}(\boldsymbol{\mu}) := \zeta_k^{Re}(\boldsymbol{\mu}) \mathbf{c}_k^{Re}$  and  $\tilde{\mathbf{e}}^{Im}(\boldsymbol{\mu}) := \zeta_k^{Im}(\boldsymbol{\mu}) \mathbf{c}_k^{Im}$ . By taking  $\mathbf{e}^{Re} = \tilde{\mathbf{e}}^{Re}$  and  $\mathbf{e}^{Im} = \tilde{\mathbf{e}}^{Im}$  in (3.6-3.7), the linear systems involving the unknowns  $\zeta_k^{Re}(\boldsymbol{\mu})$  and  $\zeta_k^{Im}(\boldsymbol{\mu})$  are as follows

$$-\gamma(\boldsymbol{\mu}) M \mathbf{c}_k^{Im} \zeta_k^{Im}(\boldsymbol{\mu}) + \sum_{j=1}^{m_a} p_j(\boldsymbol{\mu}) A_j \mathbf{c}_k^{Re} \zeta_k^{Re}(\boldsymbol{\mu}) = \mathbf{r}_k^{Re}(\boldsymbol{\mu}), \quad (3.10)$$

$$\gamma(\boldsymbol{\mu}) M \mathbf{c}_k^{Re} \zeta_k^{Re}(\boldsymbol{\mu}) + \sum_{j=1}^{m_a} p_j(\boldsymbol{\mu}) A_j \mathbf{c}_k^{Im} \zeta_k^{Im}(\boldsymbol{\mu}) = \mathbf{r}_k^{Im}(\boldsymbol{\mu}). \quad (3.11)$$

Taking the dot product of (3.10) with  $\mathbf{c}_k^{Re}$  and (3.11) with  $\mathbf{c}_k^{Im}$  yields the affine representations of  $\zeta_k^{Re}(\boldsymbol{\mu})$  and  $\zeta_k^{Im}(\boldsymbol{\mu})$  as

$$\zeta_k^{Re}(\boldsymbol{\mu}) = \frac{\sum_{j=1}^{m_a} p_j(\boldsymbol{\mu}) (\mathbf{c}_k^{Im})^T A_j \mathbf{c}_k^{Im} \cdot (\mathbf{c}_k^{Re})^T \mathbf{r}_k^{Re}(\boldsymbol{\mu}) + \gamma(\boldsymbol{\mu}) (\mathbf{c}_k^{Re})^T M \mathbf{c}_k^{Im} \cdot (\mathbf{c}_k^{Im})^T \mathbf{r}_k^{Im}(\boldsymbol{\mu})}{\sum_{j=1}^{m_a} p_j(\boldsymbol{\mu}) (\mathbf{c}_k^{Re})^T A_j \mathbf{c}_k^{Re} \cdot \sum_{j=1}^{m_a} p_j(\boldsymbol{\mu}) (\mathbf{c}_k^{Im})^T A_j \mathbf{c}_k^{Im} + \gamma(\boldsymbol{\mu}) (\mathbf{c}_k^{Re})^T M \mathbf{c}_k^{Im} \cdot \gamma(\boldsymbol{\mu}) (\mathbf{c}_k^{Im})^T M \mathbf{c}_k^{Re}}, \quad (3.12)$$

$$\zeta_k^{Im}(\boldsymbol{\mu}) = \frac{\sum_{j=1}^{m_a} p_j(\boldsymbol{\mu}) (\mathbf{c}_k^{Re})^T A_j \mathbf{c}_k^{Re} \cdot (\mathbf{c}_k^{Im})^T \mathbf{r}_k^{Im}(\boldsymbol{\mu}) - \gamma(\boldsymbol{\mu}) (\mathbf{c}_k^{Im})^T M \mathbf{c}_k^{Re} \cdot (\mathbf{c}_k^{Re})^T \mathbf{r}_k^{Re}(\boldsymbol{\mu})}{\gamma(\boldsymbol{\mu}) (\mathbf{c}_k^{Re})^T M \mathbf{c}_k^{Im} \cdot \gamma(\boldsymbol{\mu}) (\mathbf{c}_k^{Im})^T M \mathbf{c}_k^{Re} + \sum_{j=1}^{m_a} p_j(\boldsymbol{\mu}) (\mathbf{c}_k^{Im})^T A_j \mathbf{c}_k^{Im} \cdot \sum_{j=1}^{m_a} p_j(\boldsymbol{\mu}) (\mathbf{c}_k^{Re})^T A_j \mathbf{c}_k^{Re}}, \quad (3.13)$$

where both  $\mathbf{r}_k^{Re}(\boldsymbol{\mu})$  and  $\mathbf{r}_k^{Im}(\boldsymbol{\mu})$  are affine in  $\boldsymbol{\mu}$ , as defined by Eqs. (3.8)-(3.9).

The iteration procedure ends when  $|\mathbf{r}_k(\boldsymbol{\mu}_k)|$  is small enough. The above procedure of the VS method for the complex-valued elliptic problem is summarized in Algorithm 1.

We emphasize that the coefficients  $\{\mathbf{c}_j^{Re}\}_{j=1}^N$  and  $\{\mathbf{c}_j^{Im}\}_{j=1}^N$  (independent of  $\boldsymbol{\mu}$ ) can be calculated during the offline stage of the VS method, and used directly in the online stage. Then we only need to calculate the parametric functions in Eq. (3.4) for any  $\boldsymbol{\mu} \in \tilde{\Omega}$  during the online stage. This procedure is highly efficient, as it only involves the separate representation given by (3.4).

Although the VS method successfully constructs reduced-order models for frequency-domain problems, its application to time-domain dynamical problems in complex geometries remains challenging. In particular, employing the Fourier transform in such scenarios often necessitates a large  $N$  to achieve sufficient approximation accuracy, leading to high computational costs. To address this limitation and enhance computational efficiency, we propose incorporating a domain decomposition strategy.

---

**Algorithm 1** A VS method for the complex-valued elliptic problem

---

**Require:** The complex-valued elliptic problem (3.3), a set of samples  $\Xi \in \tilde{\Omega}$ , and the error tolerance  $\varepsilon$ .

**Ensure:** The approximation  $\hat{\mathbf{u}}_N(\boldsymbol{\mu}) := \sum_{j=1}^N \left( \zeta_j^{Re}(\boldsymbol{\mu}) \mathbf{c}_j^{Re} + i \zeta_j^{Im}(\boldsymbol{\mu}) \mathbf{c}_j^{Im} \right)$ .

1. Initialize the iteration counter  $k = 1$ , a random  $\boldsymbol{\mu}_1 \in \Xi$ ;
  2. Calculate  $\mathbf{c}_k^{Re}$  and  $\mathbf{c}_k^{Im}$  by solving (3.6) and (3.7) with  $\boldsymbol{\mu} = \boldsymbol{\mu}_k$ ; compute  $\zeta_k^{Re}(\boldsymbol{\mu})$  and  $\zeta_k^{Im}(\boldsymbol{\mu})$  by (3.12) and (3.13);
  3. Update  $\Xi = \Xi \setminus \boldsymbol{\mu}_k$ , and take  $\hat{\mathbf{u}}_k(x; \boldsymbol{\mu}) := \sum_{j=1}^k \left( \zeta_j^{Re}(\boldsymbol{\mu}) \mathbf{c}_j^{Re} + i \zeta_j^{Im}(\boldsymbol{\mu}) \mathbf{c}_j^{Im} \right)$ ;
  4. Set  $k \rightarrow k + 1$ ;
  5. If  $|\mathbf{r}(\boldsymbol{\mu})| \geq \varepsilon$  and  $\Xi \neq \emptyset$ , choose  $\boldsymbol{\mu}_k \in \underset{\boldsymbol{\mu} \in \Xi}{\operatorname{argmax}} |\mathbf{r}_k(\boldsymbol{\mu})|$ , and **return** to Step 2; otherwise set  $N = k$  and **terminate**.
- 

### 3.2 Domain decomposition method for complex-valued problems

In this section, we provide a brief introduction to the non-overlapping domain decomposition method for complex-valued problems. For general real-valued problems, relevant references include [42, 34]. Here the complex-valued problem (2.2) is considered for a fixed  $\bar{\boldsymbol{\mu}} \in \tilde{\Omega}$ . Suppose that the domain  $D$  is divide into  $N_s$  non-overlapping subdomains  $\{D_j\}_{j=1}^{N_s}$  such that

$$D = \bigcup_{j=1}^{N_s} \overline{D_j} \quad \text{and} \quad D_j \cap D_k = \emptyset, \quad \text{if } j \neq k.$$

Restricting the weak formulation (3.1) to a typical subdomain  $D_j$ , we obtain

$$a(\hat{\mathbf{u}}, \hat{\mathbf{v}}; \bar{\boldsymbol{\mu}})_j = b(\hat{\mathbf{v}}; \bar{\boldsymbol{\mu}})_j \quad \forall \hat{\mathbf{v}} \in \mathcal{V}_j,$$

where  $\mathcal{V}_j$  is the Hilbert space  $\mathcal{V}$  restricted on subdomain  $D_j$ . The finite element discretization of the above equation yields the following local linear system

$$A^j \hat{\mathbf{u}}^j = \mathbf{f}^j, \tag{3.14}$$

where  $A^j$ ,  $\mathbf{f}^j$ , and  $\hat{\mathbf{u}}^j$  denote the local system matrix, local load vector, and local unknown solution, respectively. All of those are complex-valued, i.e.,

$$A^j := A^{j,Re} + i A^{j,Im}, \quad \hat{\mathbf{u}}^j := \hat{\mathbf{u}}^{j,Re} + i \hat{\mathbf{u}}^{j,Im}, \quad \mathbf{f}^j := \mathbf{f}^{j,Re} + i \mathbf{f}^{j,Im}.$$

Similar to the real-valued case, the local system (3.14) is singular due to the lack of boundary conditions. To address this, we decompose  $\hat{\mathbf{u}}^j$  into two parts: the interface part  $\hat{\mathbf{u}}_\Gamma^j$ , where the nodes are shared by two or more adjacent subdomains, and the interior part  $\hat{\mathbf{u}}_I^j$  belonging to the subdomain  $D_j$ . As a result, (3.14) can be rewritten as

$$\begin{bmatrix} A_{II}^{j,Re} + i A_{II}^{j,Im} & A_{I\Gamma}^{j,Re} + i A_{I\Gamma}^{j,Im} \\ A_{\Gamma I}^{j,Re} + i A_{\Gamma I}^{j,Im} & A_{\Gamma\Gamma}^{j,Re} + i A_{\Gamma\Gamma}^{j,Im} \end{bmatrix} \begin{Bmatrix} \hat{\mathbf{u}}_I^{j,Re} + i \hat{\mathbf{u}}_I^{j,Im} \\ \hat{\mathbf{u}}_\Gamma^{j,Re} + i \hat{\mathbf{u}}_\Gamma^{j,Im} \end{Bmatrix} = \begin{Bmatrix} \mathbf{f}_I^{j,Re} + i \mathbf{f}_I^{j,Im} \\ \mathbf{f}_\Gamma^{j,Re} + i \mathbf{f}_\Gamma^{j,Im} \end{Bmatrix}.$$

The system reveals that once the interface unknowns  $\hat{\mathbf{u}}_\Gamma^j$  are determined, the interior unknowns  $\hat{\mathbf{u}}_I^j$  can be computed through the following interior problem

$$\left[ A_{II}^{j,Re} + i A_{II}^{j,Im} \right] \left\{ \hat{\mathbf{u}}_I^{j,Re} + i \hat{\mathbf{u}}_I^{j,Im} \right\} = \left\{ \mathbf{f}_I^{j,Re} + i \mathbf{f}_I^{j,Im} \right\} - \left[ A_{I\Gamma}^{j,Re} + i A_{I\Gamma}^{j,Im} \right] \left\{ \hat{\mathbf{u}}_\Gamma^{j,Re} + i \hat{\mathbf{u}}_\Gamma^{j,Im} \right\}.$$

Define the local Schur complement matrix  $S_j$  and the corresponding right-hand side vector  $F_j$  as

$$S_j = \left[ A_{\Gamma\Gamma}^{j,Re} + iA_{\Gamma\Gamma}^{j,Im} \right] - \left[ A_{\Gamma I}^{j,Re} + iA_{\Gamma I}^{j,Im} \right] \left[ A_{II}^{j,Re} + iA_{II}^{j,Im} \right]^{-1} \left[ A_{I\Gamma}^{j,Re} + iA_{I\Gamma}^{j,Im} \right],$$

$$F_j = \left\{ \mathbf{f}_{\Gamma}^{j,Re} + i\mathbf{f}_{\Gamma}^{j,Im} \right\} - \left[ A_{\Gamma I}^{j,Re} + iA_{\Gamma I}^{j,Im} \right] \left[ A_{II}^{j,Re} + iA_{II}^{j,Im} \right]^{-1} \left\{ \mathbf{f}_I^{j,Re} + i\mathbf{f}_I^{j,Im} \right\},$$

the global interface unknowns  $\hat{\mathbf{u}}_{\Gamma}$  can be obtained by solving the global interface problem

$$S\hat{\mathbf{u}}_{\Gamma} = F, \quad (3.15)$$

where

$$S := \sum_{j=1}^{N_s} R_j^T S_j R_j \quad \text{and} \quad F := \sum_{j=1}^{N_s} R_j^T F_j.$$

The restriction matrix  $R_j$  acts as a scatter operator that maps the global interface unknowns  $\hat{\mathbf{u}}_{\Gamma}$  to the local interface unknowns  $\hat{\mathbf{u}}_{\Gamma}^j$ , satisfying the relation  $R_j \hat{\mathbf{u}}_{\Gamma} = \hat{\mathbf{u}}_{\Gamma}^j$ . This operator enables the consistent transfer of interface information from the global domain to each local subdomain within the domain decomposition framework.

Note that the primary computational cost in constructing  $S$  and  $F$  arises from inverting the complex-valued matrices  $A_{II}^{j,Re} + iA_{II}^{j,Im}$ ,  $j = 1, \dots, N_s$ . In this paper, we aim to investigate the application of the domain decomposition method to parametric dynamical systems. Through the Fourier transform, these systems can be transformed into complex-valued elliptic problems that contain a large number of parameters. For each random input  $\boldsymbol{\mu} \in \tilde{\Omega}$ , all the aforementioned matrices are  $\boldsymbol{\mu}$ -dependent, introducing significant computational challenges in solving the interface system.

## 4 Domain decomposition based on variable-separation

In this section, we will first present an offline-online method for the interface problem of the complex-valued elliptic problem, which builds a relation between the random inputs and the global interface solution, in subsections 4.1-4.2. And then present the separate representations of the solutions for the subproblems in subsection 4.3. Following the previous subsection, the interface problem for the complex-valued elliptic equation can be formally expressed as (referring to Eq. (3.15)):

$$S(\boldsymbol{\mu})\hat{\mathbf{u}}_{\Gamma}(\boldsymbol{\mu}) = F(\boldsymbol{\mu}),$$

where

$$S(\boldsymbol{\mu}) := \sum_{j=1}^{N_s} R_j^T S_j(\boldsymbol{\mu}) R_j, \quad F(\boldsymbol{\mu}) := \sum_{j=1}^{N_s} R_j^T F_j(\boldsymbol{\mu}),$$

and

$$S_j(\boldsymbol{\mu}) = \left[ A_{\Gamma\Gamma}^{j,Re}(\boldsymbol{\mu}) + iA_{\Gamma\Gamma}^{j,Im}(\boldsymbol{\mu}) \right] - \left[ A_{\Gamma I}^{j,Re}(\boldsymbol{\mu}) + iA_{\Gamma I}^{j,Im}(\boldsymbol{\mu}) \right] \left[ A_{II}^{j,Re}(\boldsymbol{\mu}) + iA_{II}^{j,Im}(\boldsymbol{\mu}) \right]^{-1} \left[ A_{I\Gamma}^{j,Re}(\boldsymbol{\mu}) + iA_{I\Gamma}^{j,Im}(\boldsymbol{\mu}) \right], \quad (4.1)$$

$$F_j(\boldsymbol{\mu}) = \left\{ \mathbf{f}_{\Gamma}^{j,Re}(\boldsymbol{\mu}) + i\mathbf{f}_{\Gamma}^{j,Im}(\boldsymbol{\mu}) \right\} - \left[ A_{\Gamma I}^{j,Re}(\boldsymbol{\mu}) + iA_{\Gamma I}^{j,Im}(\boldsymbol{\mu}) \right] \left[ A_{II}^{j,Re}(\boldsymbol{\mu}) + iA_{II}^{j,Im}(\boldsymbol{\mu}) \right]^{-1} \left\{ \mathbf{f}_I^{j,Re}(\boldsymbol{\mu}) + i\mathbf{f}_I^{j,Im}(\boldsymbol{\mu}) \right\}. \quad (4.2)$$

To simplify the presentation of the methodology, we partition domain  $D$  into two subdomains  $D_1$  and  $D_2$ , denoting their interface by  $\Gamma$  (rather than  $\Gamma_{12}$ ). We emphasize that the two-subdomain analysis extends naturally to multiple subdomains. The corresponding interface problem for the complex-valued elliptic equation takes the following form

$$(S_1(\boldsymbol{\mu}) + S_2(\boldsymbol{\mu}))\hat{\mathbf{u}}_{\Gamma}(\boldsymbol{\mu}) = F_1(\boldsymbol{\mu}) + F_2(\boldsymbol{\mu}). \quad (4.3)$$

#### 4.1 Affine representations of $S$ and $F$

To enhance the computational efficiency, we develop an affine-reformulation strategy for (4.3) that guarantees the affine parameter dependence of both  $S(\boldsymbol{\mu})$  and  $F(\boldsymbol{\mu})$ . The complete implementation details of this reformulation approach are presented in this section. Using the affine decomposition (3.2), the parametric matrices defined in Eqs. (4.1)-(4.2) admit the following representation

$$\begin{aligned} A_{II}^{j,Re}(\boldsymbol{\mu}) &= \sum_{n=1}^{m_{a_j}} \alpha^{jn}(\boldsymbol{\mu}) A_{II}^{jn}, \quad A_{II}^{j,Im}(\boldsymbol{\mu}) = \gamma^j(\boldsymbol{\mu}) M_{II}^j, \\ A_{I\Gamma}^{j,Re}(\boldsymbol{\mu}) &= \sum_{n=1}^{m_{a_j}} \alpha^{jn}(\boldsymbol{\mu}) A_{I\Gamma}^{jn}, \quad A_{I\Gamma}^{j,Im}(\boldsymbol{\mu}) = \gamma^j(\boldsymbol{\mu}) M_{I\Gamma}^j, \\ A_{\Gamma I}^{j,Re}(\boldsymbol{\mu}) &= \sum_{n=1}^{m_{a_j}} \alpha^{jn}(\boldsymbol{\mu}) A_{\Gamma I}^{jn}, \quad A_{\Gamma I}^{j,Im}(\boldsymbol{\mu}) = \gamma^j(\boldsymbol{\mu}) M_{\Gamma I}^j, \\ A_{\Gamma\Gamma}^{j,Re}(\boldsymbol{\mu}) &= \sum_{n=1}^{m_{a_j}} \alpha^{jn}(\boldsymbol{\mu}) A_{\Gamma\Gamma}^{jn}, \quad A_{\Gamma\Gamma}^{j,Im}(\boldsymbol{\mu}) = \gamma^j(\boldsymbol{\mu}) M_{\Gamma\Gamma}^j, \end{aligned} \quad (4.4)$$

where the matrices  $A_{II}^{jn}$ ,  $A_{I\Gamma}^{jn}$ ,  $A_{\Gamma I}^{jn}$ ,  $A_{\Gamma\Gamma}^{jn}$  and  $M_{II}^j$ ,  $M_{I\Gamma}^j$ ,  $M_{\Gamma I}^j$ ,  $M_{\Gamma\Gamma}^j$  are all independent of  $\boldsymbol{\mu}$ . It can be seen that the first term of  $S_i(\boldsymbol{\mu})$  satisfies the structure that is affine with respect to  $\boldsymbol{\mu}$  as we desired. Next, we will discuss how to obtain the affine approximation of the second term of  $S_i(\boldsymbol{\mu})$ , i.e.,

$$- \left[ A_{\Gamma I}^{j,Re}(\boldsymbol{\mu}) + i A_{\Gamma I}^{j,Im}(\boldsymbol{\mu}) \right] \left[ A_{II}^{j,Re}(\boldsymbol{\mu}) + i A_{II}^{j,Im}(\boldsymbol{\mu}) \right]^{-1} \left[ A_{I\Gamma}^{j,Re}(\boldsymbol{\mu}) + i A_{I\Gamma}^{j,Im}(\boldsymbol{\mu}) \right].$$

- *Step 1: Construct the low-rank approximation of*

$$X^j(\boldsymbol{\mu}) = \left[ A_{II}^{j,Re}(\boldsymbol{\mu}) + i A_{II}^{j,Im}(\boldsymbol{\mu}) \right]^{-1} \left[ A_{I\Gamma}^{j,Re}(\boldsymbol{\mu}) + i A_{I\Gamma}^{j,Im}(\boldsymbol{\mu}) \right] \quad (4.5)$$

such as

$$X_N^j(\boldsymbol{\mu}) := \sum_{n=1}^{N_{S_i}} (\phi_n^{j,Re}(\boldsymbol{\mu}) X_n^{j,Re} + i \phi_n^{j,Im}(\boldsymbol{\mu}) X_n^{j,Im}). \quad (4.6)$$

Indeed, under the assumption of affine decomposition (4.4), one can rewrite (4.5) as

$$\left( \sum_{n=1}^{m_{a_j}} \alpha^{jn}(\boldsymbol{\mu}) A_{II}^{jn} + i \gamma^j(\boldsymbol{\mu}) M_{II}^j \right) X^j(\boldsymbol{\mu}) = \left( \sum_{n=1}^{m_{a_j}} \alpha^{jn}(\boldsymbol{\mu}) A_{I\Gamma}^{jn} + i \gamma^j(\boldsymbol{\mu}) M_{I\Gamma}^j \right).$$

Let  $n_\Gamma$  be the number of the interface unknowns. The unknown parametric matrix  $X^j(\boldsymbol{\mu})$  can be expressed as  $X^j(\boldsymbol{\mu}) = [x_1^j(\boldsymbol{\mu}), x_2^j(\boldsymbol{\mu}), \dots, x_{n_\Gamma}^j(\boldsymbol{\mu})]$ , and each element  $x_k^j(\boldsymbol{\mu})$ ,  $k = 1, \dots, n_\Gamma$  can be obtained by solving

$$\left( \sum_{n=1}^{m_{a_j}} \alpha^{jn}(\boldsymbol{\mu}) A_{II}^{jn} + i \gamma^j(\boldsymbol{\mu}) M_{II}^j \right) x_k^j(\boldsymbol{\mu}) = \alpha_k^j(\boldsymbol{\mu}), \quad (4.7)$$

where  $\alpha_k^j$  represents the  $k$ -th column of the matrix  $\left( \sum_{n=1}^{m_{a_j}} \alpha^{jn}(\boldsymbol{\mu}) A_{I\Gamma}^{jn} + i \gamma^j(\boldsymbol{\mu}) M_{I\Gamma}^j \right)$ .

By applying Algorithm 1 from subsection 3.1, we are able to derive the low-rank approximation for each component  $x_k^j(\boldsymbol{\mu})$ . Then, the approximate solution  $X_N^j(\boldsymbol{\mu})$  in Eq. (4.6) is constructed by rearranging the low-rank approximations of  $\{x_k^i(\boldsymbol{\mu})\}_{k=1}^{n_\Gamma}$ .

- *Step 2: Assemble affine expression for*

$$\mathcal{X}^j(\boldsymbol{\mu}) = - \left[ A_{\Gamma I}^{j,Re}(\boldsymbol{\mu}) + i A_{\Gamma I}^{j,Im}(\boldsymbol{\mu}) \right] \left[ A_{II}^{j,Re}(\boldsymbol{\mu}) + i A_{II}^{j,Im}(\boldsymbol{\mu}) \right]^{-1} \left[ A_{I\Gamma}^{j,Re}(\boldsymbol{\mu}) + i A_{I\Gamma}^{j,Im}(\boldsymbol{\mu}) \right].$$

Based on the low-rank representation of  $X^j(\boldsymbol{\mu})$  and Eq. (4.4), we have

$$\begin{aligned}\mathcal{X}^j(\boldsymbol{\mu}) &\approx -\left[\sum_{n=1}^{m_{a_j}} \alpha^{jn}(\boldsymbol{\mu}) A_{\Gamma I}^{jn} + i\gamma^j(\boldsymbol{\mu}) M_{\Gamma I}^j\right] \left[\sum_{n=1}^{N_{S_i}} (\phi_n^{j,Re}(\boldsymbol{\mu}) X_n^{j,Re} + i\phi_n^{j,Im}(\boldsymbol{\mu}) X_n^{j,Im})\right] \\ &= \sum_{n=1}^{(m_{a_j}+1)N_{S_i}} (\eta_n^{j,Re}(\boldsymbol{\mu}) \mathcal{X}_n^{j,Re} + i\eta_n^{j,Im}(\boldsymbol{\mu}) \mathcal{X}_n^{j,Im}),\end{aligned}\quad (4.8)$$

in which

$$\begin{cases} \eta_n^{j,Re}(\boldsymbol{\mu}) = \alpha^{jn_1}(\boldsymbol{\mu}) \phi_{n_2}^{j,Re}(\boldsymbol{\mu}), & \mathcal{X}_n^{j,Re} = A_{\Gamma I}^{jn_1} X_{n_2}^{j,Re}, \\ \eta_n^{j,Im}(\boldsymbol{\mu}) = \alpha^{jn_1}(\boldsymbol{\mu}) \phi_{n_2}^{j,Im}(\boldsymbol{\mu}), & \mathcal{X}_n^{j,Im} = A_{\Gamma I}^{jn_1} X_{n_2}^{j,Im}, \end{cases} \quad n = 1, 2, \dots, m_{a_j} N_{S_j},$$

and

$$\begin{cases} \eta_n^{j,Re}(\boldsymbol{\mu}) = \gamma^j(\boldsymbol{\mu}) \phi_{n_2}^{j,Im}(\boldsymbol{\mu}), & \mathcal{X}_n^{j,Re} = -M_{\Gamma I}^j X_{n_2}^{j,Im}, \\ \eta_n^{j,Im}(\boldsymbol{\mu}) = \gamma^j(\boldsymbol{\mu}) \phi_{n_2}^{j,Re}(\boldsymbol{\mu}), & \mathcal{X}_n^{j,Im} = M_{\Gamma I}^j X_{n_2}^{j,Re}, \end{cases} \quad n = m_{a_j} N_{S_j} + 1, \dots, (m_{a_j} + 1) N_{S_i},$$

where  $n_1 = 1, 2, \dots, m_{a_j}$  and  $n_2 = 1, 2, \dots, N_{S_j}$ .

Subsequently, the low-rank representation for  $S_j(\boldsymbol{\mu})$  in Eq. (4.1) is expressed as

$$\begin{aligned}S_j(\boldsymbol{\mu}) &= \left[A_{\Gamma\Gamma}^{j,Re}(\boldsymbol{\mu}) + iA_{\Gamma\Gamma}^{j,Im}(\boldsymbol{\mu})\right] + \mathcal{X}^j(\boldsymbol{\mu}) \\ &\approx \sum_{n=1}^{m_{a_j}} \alpha^{jn}(\boldsymbol{\mu}) A_{\Gamma\Gamma}^{jn} + i\gamma^j(\boldsymbol{\mu}) M_{\Gamma\Gamma}^j + \sum_{n=1}^{(m_{a_j}+1)N_{S_i}} (\eta_n^{j,Re}(\boldsymbol{\mu}) \mathcal{X}_n^{j,Re} + i\eta_n^{j,Im}(\boldsymbol{\mu}) \mathcal{X}_n^{j,Im}).\end{aligned}$$

Finally, we have the low-rank representation for  $S(\boldsymbol{\mu})$  as follows

$$S(\boldsymbol{\mu}) = S_1(\boldsymbol{\mu}) + S_2(\boldsymbol{\mu}) \approx \sum_{n=1}^{m_S} \left(\hat{\eta}_n^{Re}(\boldsymbol{\mu}) \hat{\mathcal{X}}_n^{Re} + i\hat{\eta}_n^{Im}(\boldsymbol{\mu}) \hat{\mathcal{X}}_n^{Im}\right), \quad (4.9)$$

where the sum term comes from stacking the variables and sorting the corresponding indices via a single one, and  $m_S = m_{a_1} + m_{a_2} + (m_{a_1} + 1)N_{S_1} + (m_{a_2} + 1)N_{S_2}$ . We note that  $m_S$  is the number of the real part of  $S(\boldsymbol{\mu})$ , and the number of its imaginary part is equal to  $2 + (m_{a_1} + 1)N_{S_1} + (m_{a_2} + 1)N_{S_2}$ , which is less than or equal to  $m_S$ . For convenience, we also use  $m_S$  to denote the number of the imaginary part. Because the terms with index  $n = 3 + (m_{a_1} + 1)N_{S_1} + (m_{a_2} + 1)N_{S_2}, \dots, m_S$  for the imaginary part can be set as 0.

Algorithm 2 outlines the assembling process of  $S(\boldsymbol{\xi})$ .

Similarly, with the assumption (3.2) of affine decomposition, we have

$$\begin{aligned}\mathbf{f}_I^{j,Re}(\boldsymbol{\mu}) &= \sum_{n=1}^{m_{b_i}} \beta^{jn,Re}(\boldsymbol{\mu}) \mathbf{f}_I^{jn,Re}, & \mathbf{f}_I^{j,Im}(\boldsymbol{\mu}) &= \sum_{n=1}^{m_{b_i}} \beta^{jn,Im}(\boldsymbol{\mu}) \mathbf{f}_I^{jn,Im}, \\ \mathbf{f}_\Gamma^{j,Re}(\boldsymbol{\mu}) &= \sum_{n=1}^{m_{b_i}} \beta^{jn,Re}(\boldsymbol{\mu}) \mathbf{f}_\Gamma^{jn,Re}, & \mathbf{f}_\Gamma^{j,Im}(\boldsymbol{\mu}) &= \sum_{n=1}^{m_{b_i}} \beta^{jn,Im}(\boldsymbol{\mu}) \mathbf{f}_\Gamma^{jn,Im},\end{aligned}\quad (4.10)$$

where  $\mathbf{f}_I^{jn,Re}$ ,  $\mathbf{f}_I^{jn,Im}$ ,  $\mathbf{f}_\Gamma^{jn,Re}$  and  $\mathbf{f}_\Gamma^{jn,Im}$  are independent of  $\boldsymbol{\mu}$ . Following the assemble strategy of  $S(\boldsymbol{\mu})$ , one can derive the low-rank representation for  $F(\boldsymbol{\mu})$  as follows

$$F(\boldsymbol{\mu}) = F_1(\boldsymbol{\mu}) + F_2(\boldsymbol{\mu}) \approx \sum_{n=1}^{m_F} \left(\hat{\rho}_n^{Re}(\boldsymbol{\mu}) \hat{F}_n^{Re} + i\hat{\rho}_n^{Im}(\boldsymbol{\mu}) \hat{F}_n^{Im}\right), \quad (4.11)$$

where  $m_F = m_{b_1} + m_{b_2} + (m_{a_1} + 1)N_{F_1} + (m_{a_2} + 1)N_{F_2}$ . The detailed procedure of assembling  $F(\boldsymbol{\mu})$  is pretend in Algorithm 3.

---

**Algorithm 2** The Assemble Process of  $S(\boldsymbol{\mu})$ 

---

**Require:** The complex-valued matrices  $A_{II}^j(\boldsymbol{\mu})$ ,  $A_{I\Gamma}^j(\boldsymbol{\mu})$ ,  $A_{\Gamma I}^j(\boldsymbol{\mu})$ ,  $A_{\Gamma\Gamma}^j(\boldsymbol{\mu})$ ,  $j = 1, 2$ .

**Ensure:** The low-rank representation  $S(\boldsymbol{\mu}) = \sum_{n=1}^{m_S} \left( \hat{\eta}_n^{Re}(\boldsymbol{\mu}) \hat{\chi}_n^{Re} + i \hat{\eta}_n^{Im}(\boldsymbol{\mu}) \hat{\chi}_n^{Im} \right)$ .

1. Get the approximation of

$$X(\boldsymbol{\mu}) = \left[ A_{II}^{j,Re}(\boldsymbol{\mu}) + i A_{II}^{j,Im}(\boldsymbol{\mu}) \right]^{-1} \left[ A_{I\Gamma}^{j,Re}(\boldsymbol{\mu}) + i A_{I\Gamma}^{j,Im}(\boldsymbol{\mu}) \right]$$

by solving Eq. (4.7) with Algorithm 1;

2. Assemble the affine expression of

$$- \left[ A_{\Gamma I}^{j,Re}(\boldsymbol{\mu}) + i A_{\Gamma I}^{j,Im}(\boldsymbol{\mu}) \right] \left[ A_{II}^{j,Re}(\boldsymbol{\mu}) + i A_{II}^{j,Im}(\boldsymbol{\mu}) \right]^{-1} \left[ A_{I\Gamma}^{j,Re}(\boldsymbol{\mu}) + i A_{I\Gamma}^{j,Im}(\boldsymbol{\mu}) \right]$$

by (4.8);

3. Assemble  $S_j(\boldsymbol{\mu})$  based on (4.4) and the expression derived in Step 2;
  4. Assemble the low-rank representation of  $S(\boldsymbol{\mu})$  by (4.9).
- 

---

**Algorithm 3** The Assemble Process of  $F(\boldsymbol{\mu})$ 

---

**Require:** The complex-valued matrices  $A_{II}^j(\boldsymbol{\mu})$ ,  $A_{\Gamma I}^j(\boldsymbol{\mu})$  and vectors  $\mathbf{f}_I^j(\boldsymbol{\mu})$ ,  $\mathbf{f}_\Gamma^j(\boldsymbol{\mu})$ ,  $j = 1, 2$ .

**Ensure:** The low-rank representation  $F(\boldsymbol{\mu}) = \sum_{n=1}^{m_F} \left( \hat{\rho}_n^{Re}(\boldsymbol{\mu}) \hat{F}_n^{Re} + i \hat{\rho}_n^{Im}(\boldsymbol{\mu}) \hat{F}_n^{Im} \right)$ .

1. Get the approximation of  $X(\boldsymbol{\mu}) = \left[ A_{II}^{j,Re}(\boldsymbol{\mu}) + i A_{II}^{j,Im}(\boldsymbol{\mu}) \right]^{-1} \left\{ \mathbf{f}_I^{j,Re}(\boldsymbol{\mu}) + i \mathbf{f}_I^{j,Im}(\boldsymbol{\mu}) \right\}$  by Algorithm 1;
2. Assemble the affine expression of

$$- \left[ A_{\Gamma I}^{j,Re}(\boldsymbol{\mu}) + i A_{\Gamma I}^{j,Im}(\boldsymbol{\mu}) \right] \left[ A_{II}^{j,Re}(\boldsymbol{\mu}) + i A_{II}^{j,Im}(\boldsymbol{\mu}) \right]^{-1} \left\{ \mathbf{f}_I^{j,Re}(\boldsymbol{\mu}) + i \mathbf{f}_I^{j,Im}(\boldsymbol{\mu}) \right\};$$

3. Assemble  $F_j(\boldsymbol{\mu})$  based on (4.10) and the expression derived in Step 2;
  4. Assemble the low-rank representation of  $F(\boldsymbol{\mu})$  by (4.11).
-

## 4.2 Reduced model for the interface problem

Based on the separate approximations of  $S(\boldsymbol{\mu})$  and  $F(\boldsymbol{\mu})$  derived in subsection 4.1, the interface problem (4.3) can be expressed as

$$\sum_{n=1}^{m_S} \left( \hat{\eta}_n^{Re}(\boldsymbol{\mu}) \hat{\chi}_n^{Re} + i \hat{\eta}_n^{Im}(\boldsymbol{\mu}) \hat{\chi}_n^{Im} \right) \hat{\mathbf{u}}_\Gamma(\boldsymbol{\mu}) = \sum_{n=1}^{m_F} \left( \hat{\rho}_n^{Re}(\boldsymbol{\mu}) \hat{F}_n^{Re} + i \hat{\rho}_n^{Im}(\boldsymbol{\mu}) \hat{F}_n^{Im} \right), \quad (4.12)$$

which is a linear complex-valued system with  $n_\Gamma$  unknowns. Although solving (4.12) requires much less computation effort than that of the original model (4.3), this may not be a very small-scale problem. This persistence stems from the fact that the reformulated model (4.12) inherits the discretization-dependent characteristics of the original full-order system. Therefore, we further employ the VS method presented in Section 3.1 to derive the reduced model representation of the interface problem in the form of

$$\hat{\mathbf{u}}_\Gamma(\boldsymbol{\mu}) \approx \sum_{k=1}^{N_\Gamma} \left( \zeta_\Gamma^{k,Re}(\boldsymbol{\mu}) \mathbf{c}_\Gamma^{k,Re} + i \zeta_\Gamma^{k,Im}(\boldsymbol{\mu}) \mathbf{c}_\Gamma^{k,Im} \right), \quad (4.13)$$

where  $N_\Gamma$  is the number of the separate terms,  $\mathbf{c}_\Gamma^{k,Re}$  and  $\mathbf{c}_\Gamma^{k,Im}$ ,  $k = 1, \dots, N_\Gamma$  are  $n_\Gamma$ -dimension vectors. Based on this separate representation, for new random inputs, we can directly obtain the solution to the interface problem without solving (4.3) or (4.12) again. This approach has the potential of very high efficiency, as it only requires computing the coefficients  $\zeta_\Gamma^{k,Re}(\boldsymbol{\mu})$  and  $\zeta_\Gamma^{k,Im}(\boldsymbol{\mu})$  for new parameter values while reusing the precomputed spatial basis  $\mathbf{c}_\Gamma^{k,Re}$  and  $\mathbf{c}_\Gamma^{k,Im}$ .

## 4.3 Reduced model for subdomain problems

As described in subsection 3.2, once having the solution  $\hat{\mathbf{u}}_\Gamma^j(\boldsymbol{\mu})$  of the interface problem, the interior solution  $\hat{\mathbf{u}}_I^j(\boldsymbol{\mu})$  in the subdomain  $D_j$ ,  $j = 1, 2$  can be obtained by solving

$$\begin{aligned} & \left[ A_{II}^{j,Re}(\boldsymbol{\mu}) + i A_{II}^{j,Im}(\boldsymbol{\mu}) \right] \left\{ \hat{\mathbf{u}}_I^{j,Re}(\boldsymbol{\mu}) + i \hat{\mathbf{u}}_I^{j,Im}(\boldsymbol{\mu}) \right\} \\ &= \left\{ \mathbf{f}_I^{j,Re}(\boldsymbol{\mu}) + i \mathbf{f}_I^{j,Im}(\boldsymbol{\mu}) \right\} - \left[ A_{IT}^{j,Re}(\boldsymbol{\mu}) + i A_{IT}^{j,Im}(\boldsymbol{\mu}) \right] \left\{ \hat{\mathbf{u}}_\Gamma^{j,Re}(\boldsymbol{\mu}) + i \hat{\mathbf{u}}_\Gamma^{j,Im}(\boldsymbol{\mu}) \right\}, \end{aligned}$$

which is a complex-valued equation. To reduce the computational cost, we apply the VS method to construct an efficient surrogate model. Under the affine decomposition of  $A_{II}^{j,Re}(\boldsymbol{\mu})$ ,  $A_{II}^{j,Im}(\boldsymbol{\mu})$ ,  $A_{IT}^{j,Re}(\boldsymbol{\mu})$ ,  $A_{IT}^{j,Im}(\boldsymbol{\mu})$ ,  $\mathbf{f}_I^{j,Re}(\boldsymbol{\mu})$ ,  $\mathbf{f}_I^{j,Im}(\boldsymbol{\mu})$  in equation (4.4) and the affine surrogate model of the interface solutions  $\hat{\mathbf{u}}_\Gamma^{j,Re}(\boldsymbol{\mu})$ ,  $\hat{\mathbf{u}}_\Gamma^{j,Im}(\boldsymbol{\mu})$  in equation (4.13), we can derive

$$\hat{\mathbf{u}}_I^j(\boldsymbol{\mu}) \approx \sum_{k=1}^{N_I} \left( \zeta_I^{jk,Re}(\boldsymbol{\mu}) \mathbf{c}_I^{jk,Re} + i \zeta_I^{jk,Im}(\boldsymbol{\mu}) \mathbf{c}_I^{jk,Im} \right),$$

where  $N_I$  is the number of the separate terms,  $\mathbf{c}_I^{jk,Re}$  and  $\mathbf{c}_I^{jk,Im}$ ,  $k = 1, \dots, N_I$  are vectors independent of  $\boldsymbol{\mu}$ .

In summary, for time-dependent problems, after computing the corresponding solutions using the preconstructed surrogate models for both the interface problem and subproblems with new parameter inputs, we can obtain the temporal solution through an inverse Fourier transform. The entire computational process is independent of the spatial discretization of the original system and requires no time-stepping iterations, thus demonstrating remarkable efficiency.

Notably, the online stage of the proposed approach can be much more efficient. Since the surrogate models of the interface problem and subproblems, as well as their real and imaginary parts, this allows parallel computation across various frequency values.

## 5 Numerical experiments

In this section, we present three numerical examples and the corresponding numerical results to demonstrate the applicability and efficiency of the proposed method. In Sect. 5.1, the proposed VS method is applied to the heat equation. Then, we extend the proposed method to the reaction diffusion equation in Sect. 5.2.1 and Sect. 5.2.2 with different setting.

To quantify the accuracy of the proposed method, the average relative error  $\epsilon_u$  for the solution of the original dynamical systems is defined as

$$\epsilon_u := \frac{1}{M} \sum_{k=1}^M \frac{\|u(\mathbf{x}, t; \boldsymbol{\xi}_k) - u_N(\mathbf{x}, t; \boldsymbol{\xi}_k)\|_{L^2([0, T]; \mathcal{V}_h)}}{\|u(\mathbf{x}, t; \boldsymbol{\xi}_k)\|_{L^2([0, T]; \mathcal{V}_h)}}, \quad (5.1)$$

where  $M$  is the number of samples,  $u_N(\mathbf{x}, t; \boldsymbol{\xi}_k)$  is the approximate solution obtained by the proposed method (denoted FT-DD-VS), and  $u(\mathbf{x}, t; \boldsymbol{\xi}_k)$  is the reference solution. In the following numerical examples, the reference solution is calculated using FEM in space and the backward Euler scheme in time (denoted FEM-BE).

Furthermore, we define the average relative error  $\epsilon_{\hat{\mathbf{u}}}$  for the complex-valued vector as

$$\epsilon_{\hat{\mathbf{u}}} := \frac{1}{M} \sum_{k=1}^M \frac{|\hat{\mathbf{u}}(\boldsymbol{\mu}_k) - \hat{\mathbf{u}}_N(\boldsymbol{\mu}_k)|}{|\hat{\mathbf{u}}(\boldsymbol{\mu}_k)|}, \quad (5.2)$$

where  $\hat{\mathbf{u}}_N(\boldsymbol{\mu}_k)$  is the approximate solution obtained by the VS method described in subsection 3.1,  $\hat{\mathbf{u}}(\boldsymbol{\mu}_k)$  represents the reference solution computed by FEM.

### 5.1 Heat equation

In this section, we consider the following heat equation defined on domain  $D = [0, 1] \times [0, 1]$

$$\frac{\partial u}{\partial t}(\mathbf{x}, t; \boldsymbol{\xi}) - \nabla \cdot (c(\mathbf{x}; \boldsymbol{\xi}) \nabla u(\mathbf{x}, t; \boldsymbol{\xi})) = f(\mathbf{x}, t; \boldsymbol{\xi}),$$

where

$$\begin{cases} u(\mathbf{x}, 0; \boldsymbol{\xi}) = 0, & (\mathbf{x}, \boldsymbol{\xi}) \in D \times \Omega, \\ u(\mathbf{x}, t; \boldsymbol{\xi}) = 0, & (\mathbf{x}, t; \boldsymbol{\xi}) \in \partial D \times [0, T] \times \Omega. \end{cases} \quad (5.3)$$

The analytical solution of this problem is given by

$$u(\mathbf{x}, t; \boldsymbol{\xi}) = \frac{1}{\pi} \frac{t}{t^2 + 1} \sin \pi x_1 \sin \pi x_2.$$

Then, we have the source function

$$f(\mathbf{x}, t; \boldsymbol{\xi}) = \left( \frac{1}{\pi} \frac{1 - t^2}{(t^2 + 1)^2} + 2\pi \frac{t}{t^2 + 1} c(\mathbf{x}; \boldsymbol{\xi}) \right) \sin \pi x_1 \sin \pi x_2.$$

In this problem, the original domain  $D$  is divided into two subdomains  $D_1 = [0, 0.5] \times [0, 1]$  and  $D_2 = [0.5, 1] \times [0, 1]$ , and the coefficient  $c(\mathbf{x}; \boldsymbol{\xi})$  is defined as

$$c(\mathbf{x}; \boldsymbol{\xi}) = \begin{cases} \xi_1, & \mathbf{x} \in D_1, \\ 2\xi_2, & \mathbf{x} \in D_2. \end{cases}$$

Therefore, the formulations of source function in two subdomains are different. Here, the parameter  $\boldsymbol{\xi} := (\xi_1, \xi_2) \in [1, 2]^2$ . The reference solution is obtained using FEM in space with a mesh size  $h = 0.02$  and the backward Euler scheme in time with a step size  $\tau = 5 \times 10^{-4}$ .  $|\Xi|$  denotes the cardinality of the sample set  $\Xi$  and is set as  $|\Xi| = 10$  for the offline stage in Algorithm 1. In this problem, we take  $\omega^* = 20$  and  $N_\omega = 20$ , which is sufficient to derive an effective approximation.

First, we quantify the assembly errors for  $S$  and  $F$  in Step 1, which coincide with their affine approximation errors. Taking  $S_1$  as an example, Figure 1 plots the average relative error versus the number of separate terms  $N_{S_1}$ , calculated by Eq. (5.2) with  $10^3$  samples. As shown in Fig. 1, the error decreases monotonically as  $N_{S_1}$  increases, eventually falling below  $10^{-6}$ . This implies that the VS method effectively approximates complex-valued problems. To construct an efficient surrogate model for the interface problem, we select  $N_{S_1} = 4$ , ensuring the relative approximation error of  $S_1$  remains below  $10^{-6}$ . Correspondingly, we set  $N_{S_2} = 4$ ,  $N_{F_1} = 4$ , and  $N_{F_2} = 4$ .

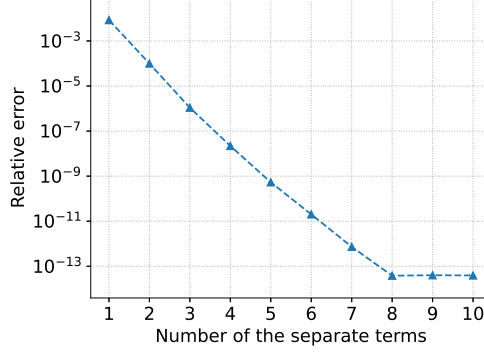


Figure 1: Average relative error versus the number of separate terms  $N_{S_1}$ .

Based on the affine approximations of  $S$  and  $F$ , Figure 2 shows the average relative error versus the number of separate terms for (a)  $M_\Gamma$  (interface problem) and (b)  $M_I$  (subdomain problems). Here, the errors  $\epsilon_{u_\Gamma}$  and  $\epsilon_{u_I}$  are calculated by Eq. (5.2) with  $10^3$  samples. We find

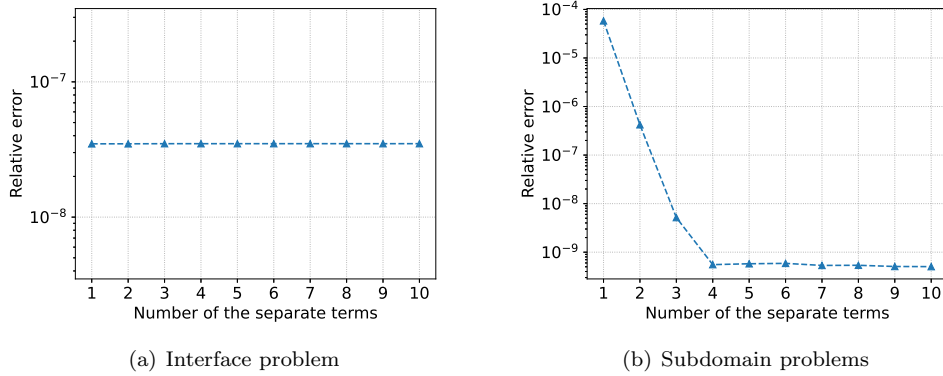


Figure 2: Average relative error versus the number of separate terms.

that the relative error of subdomain problems decreases rapidly and stabilizes when  $N_I \geq 4$ . The results demonstrate that the VS method yields accurate approximations for both interface and subdomain solutions, a capability critical for ensuring the reliability of our proposed method in parametric dynamical systems.

As evidenced by Fig. 2, the number of separate terms  $N_\Gamma = 1$  for the interface problem and  $N_I = 4$  for the subdomain problems yields a surrogate model with the desired relative error while maintaining computational efficiency. Under this configuration ( $N_\Gamma = 1$  and  $N_I = 4$ ), Fig. 3 (a) illustrates the relative errors of the first 100 samples. Along with the temporal evolution, the relative error decreases, as shown in Fig. 3 (b). From the figures, we know that the proposed method can provide a good approximation for the solution of the original problem.

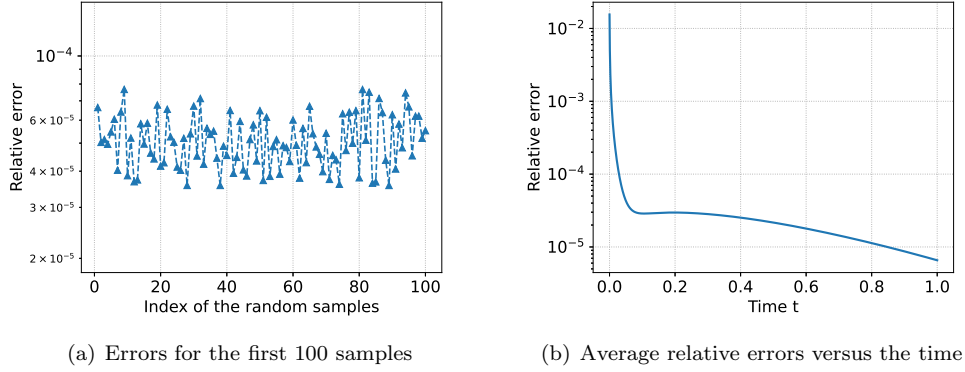


Figure 3: Comparison of the errors.

Table 1: Comparison of the average relative error and online CPU time for FT-DD-VS and FEM-BE.

Algorithm	Error $\epsilon$	Online time
FT-DD-VS	$5.05 \times 10^{-5}$	$9.39 \times 10^{-1}s$
FEM-BE	\	$3.98 \times 10^2s$

Figure 4 presents the mean solutions at  $t = 1$ , computed by the proposed method and the FEM-BE scheme in two subdomains. The top row shows the reference solutions, while the bottom row displays the corresponding results obtained using the proposed approach. It can be observed that the solution profiles and magnitudes produced by the proposed method closely match those of the reference.

In Table 1, we list the average relative error and the average online CPU time based on  $M = 10^3$  random samples. The magnitude of the average online CPU time by the proposed method is much smaller than that of the FEM-BE method. It demonstrates that the proposed method can achieve a good trade-off in both approximation accuracy and computational efficiency for this numerical experiment.

## 5.2 Reaction diffusion equation

In this subsection, we consider the reaction diffusion equation as

$$\frac{\partial u}{\partial t}(\mathbf{x}, t; \boldsymbol{\xi}) = \nabla \cdot (c_1(\mathbf{x}; \boldsymbol{\xi}) \nabla u(\mathbf{x}, t; \boldsymbol{\xi})) - c_2(\mathbf{x}; \boldsymbol{\xi}) u(\mathbf{x}, t; \boldsymbol{\xi}) + f(\mathbf{x}, t; \boldsymbol{\xi}), \quad (5.4)$$

where initial condition and homogeneous Dirichlet boundary conditions are given by Eq. (5.3). The original domain  $D = [0, 1] \times [0, 1]$  is divided into two subdomains  $D_1 = [0, 0.5] \times [0, 1]$  and  $D_2 = [0.5, 1] \times [0, 1]$ .

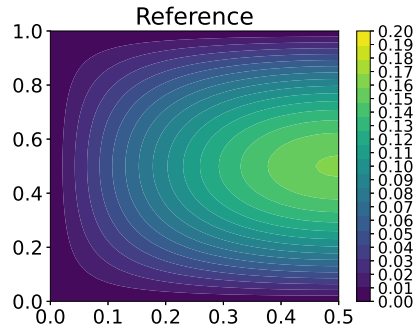
### 5.2.1 The first equation

First, we define the source function

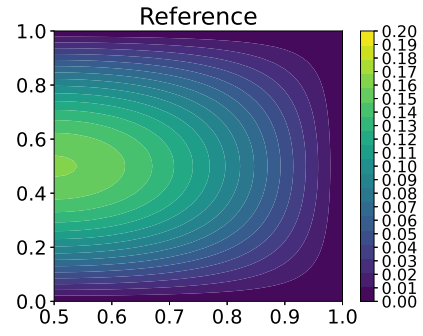
$$f(\mathbf{x}, t; \boldsymbol{\xi}) = e^{-t^2} e^{5(x_1+x_2)^2},$$

and the coefficients

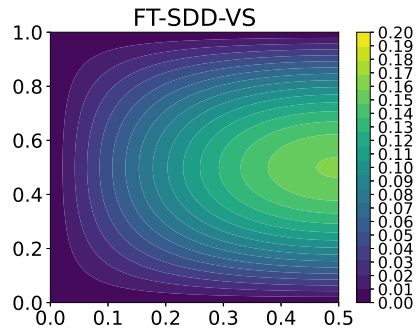
$$c_1(\mathbf{x}; \boldsymbol{\xi}) = \begin{cases} 100\xi_1, & \mathbf{x} \in D_1, \\ 10\xi_2, & \mathbf{x} \in D_2, \end{cases} \quad \text{and} \quad c_2(\mathbf{x}; \boldsymbol{\xi}) = \begin{cases} \xi_3, & \mathbf{x} \in D_1, \\ 0.1\xi_4, & \mathbf{x} \in D_2. \end{cases}$$



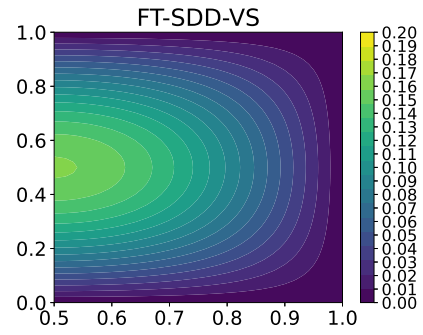
(a)  $D_1$



(b)  $D_2$



(c)  $D_1$



(d)  $D_2$

Figure 4: Comparison of the solutions in subdomains for the FEM-BE and the FT-DD-VS method.

Here, the parameter  $\xi := (\xi_1, \xi_2, \xi_3, \xi_4) \in [1, 2]^4$ . The reference solution is calculated using FEM in space with a mesh size  $h = 0.05$  and the backward Euler scheme in time with a step size  $\tau = 5 \times 10^{-4}$ . We take  $\omega^* = 15$ ,  $N_\omega = 15$ , and  $|\Xi| = 10$  for training in the offline stage of Algorithm 1. In this problem, we select  $N_{S_1} = N_{S_2} = N_{F_1} = N_{F_2} = 4$  and focus on the results of the interface problem and the subproblems.

Figure 5 plots the average relative errors of the interface problem and the subproblems against the number of the separate terms  $N$ , where the average relative errors are computed based on  $10^3$  samples. The relative error decreases as the number of separate terms increases, as shown in Fig. 5 (a) for the interface problems. For the subdomain problems, the relative error stabilizes when the number of separate terms is no less than 2. From the figures, we can see that as the number of the separate terms increases, the approximation first becomes more accurate and then stable.

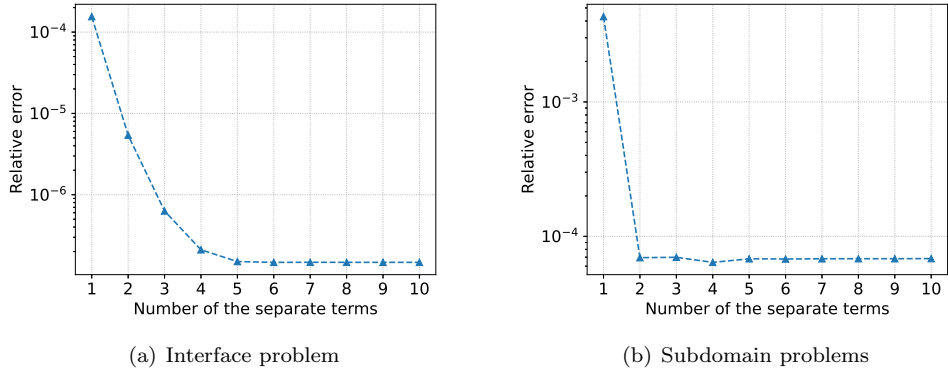


Figure 5: Average relative error versus the number of separate terms.

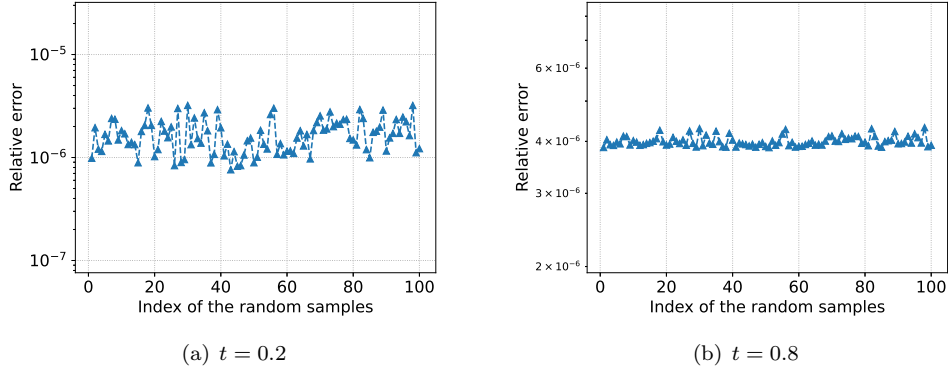


Figure 6: Errors for the first 100 samples.

To illustrate the individual relative error of the approximation in Figure 6, we set  $N_\Gamma = 3$  and  $N_I = 2$ . Fig. 6 demonstrates the relative errors of the first 100 samples at  $t = 0.2$  and  $t = 0.8$ . The range of the relative errors against the sample index at  $t = 0.2$  is wider than that at  $t = 0.8$ . Besides, we also plot the average relative errors versus different time levels in Figure 7. Here, the relative error first decreases and then increases one order of magnitude compared to that at  $t = 0.6$ . This illustrates the proposed method can provide a good approximation for the original problem (5.4) after  $t = 0.02$  with the relative error less than  $10^{-5}$ .

Finally, we present the average relative error of the proposed method, along with the average online CPU times for both the proposed method and the FEM-BE method in Table 2. The

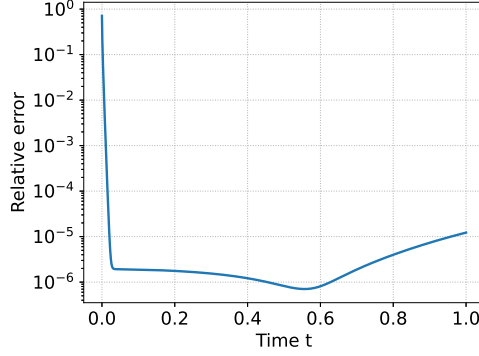


Figure 7: Average relative errors versus different time levels.

CPU time is reduced from  $7.56 \times 10^1$  to  $2.48 \times 10^{-1}$  using the proposed method, which provides a three-order-of-magnitude improvement. As shown in the table, the proposed method achieves higher accuracy with significantly lower computational cost compared to the FEM-BE method.

Table 2: Comparison of the average relative error and online CPU time for FT-DD-VS and FEM-BE.

Algorithm	Error $\epsilon$	Online time
FT-DD-VS	$9.04 \times 10^{-4}$	$2.48 \times 10^{-1}s$
FEM-BE	\	$7.56 \times 10^1s$

### 5.2.2 The second equation

In this subsection, we specify

$$f(\mathbf{x}, t; \boldsymbol{\xi}) = \frac{1 - t^2}{(1 + t^2)^2} e^{5(x_1 + x_2)^2},$$

with coefficients  $c_1(\mathbf{x}; \boldsymbol{\xi})$  and  $c_2(\mathbf{x}; \boldsymbol{\xi})$  given by

$$c_1(\mathbf{x}; \boldsymbol{\xi}) = \begin{cases} 0, & \mathbf{x} \in D_1, \\ 10\xi_1, & \mathbf{x} \in D_2, \end{cases} \quad \text{and} \quad c_2(\mathbf{x}; \boldsymbol{\xi}) = \begin{cases} 100\xi_2, & \mathbf{x} \in D_1, \\ 0, & \mathbf{x} \in D_2. \end{cases}$$

Here, the parameter  $\boldsymbol{\xi} := (\xi_1, \xi_2) \in [3, 4]^2$ . The reference solution is calculated using FEM in space with a mesh size  $h = 0.05$  and the backward Euler scheme in time with a step size  $\tau = 10^{-3}$ . In this problem, we take  $\omega^* = 15$ ,  $N_\omega = 15$ ,  $|\Xi| = 10$ , and set  $N_{S_1} = N_{S_2} = N_{F_1} = N_{F_2} = 4$ .

Figure 8 presents the average relative errors of the interface problem and the subproblems against the number of the separation terms  $N$ . The average relative errors are calculated from  $10^3$  random samples. The figures show that the approximation accuracy for the interface problem improves as  $N$  increases. However, the error of the subproblems first decreases and then plateaus as  $N$  increases. Based on the results, we set  $N_\Gamma = N_I = 4$  to perform the Fourier inversion and ensure the approximation accuracy.

To illustrate the approximation accuracy, the relative errors of the first 100 samples along with the errors versus the time are plotted in Figure 9. The results in Fig. 9 (a) demonstrate that the proposed method provides accurate approximations for the first 100 random samples. Because the curve of relative errors fluctuates around the baseline value of  $10^{-3}$ . The average

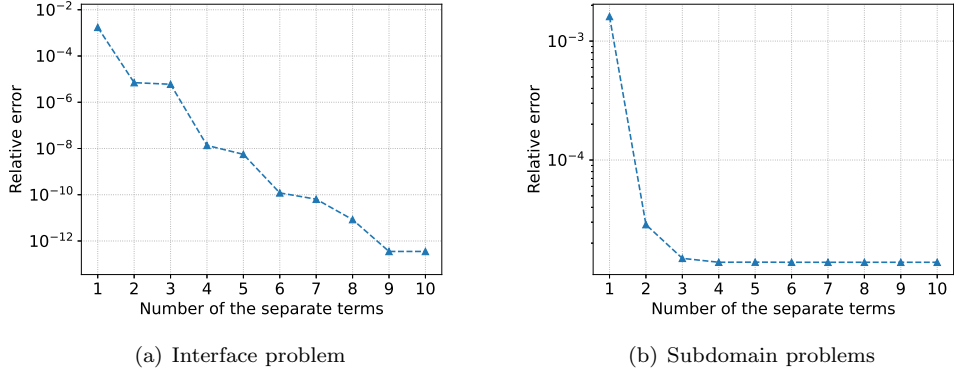


Figure 8: Average relative error versus the number of separate terms.

relative errors versus the time is shown in Fig. 9 (b). The relative errors within  $t \in [0.1, 0.9]$  exhibits a clear periodic variation pattern. Moreover, the average relative errors lies in the interval  $[10^{-6}, 10^{-4}]$  when  $t \in [0.02, 0.99]$ . In this example, the proposed method shows a good performance for  $t \in [0.02, 0.96]$ .

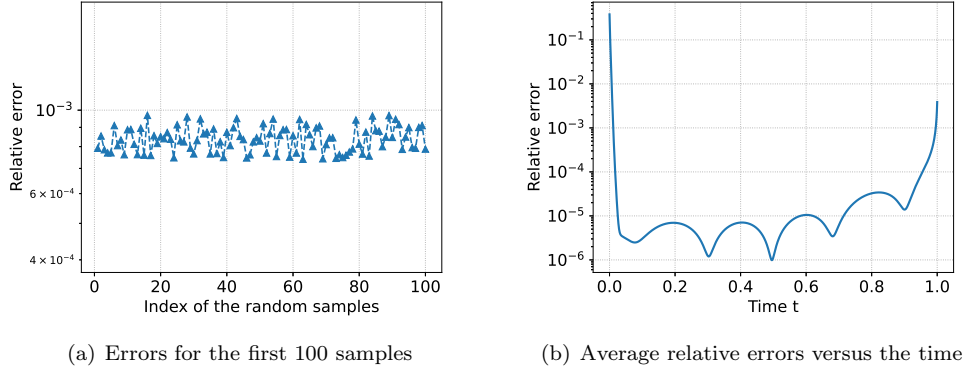


Figure 9: Comparison of the errors.

Finally, Table 3 compares the proposed method with the FEM-BE approach in terms of average relative error and computational cost. We find that the average relative error achieves an order of magnitude of  $10^{-4}$ . Moreover, the CPU time of the proposed method is orders of magnitude smaller than that of the FEM-BE method. The results demonstrate that the proposed method maintains high accuracy while achieving significant computational time reduction compared to the FEM-BE approach.

Table 3: Comparison of the average relative error and online CPU time for FT-DD-VS and FEM-BE.

Algorithm	Error $\epsilon$	Online time
FT-DD-VS	$8.40 \times 10^{-4}$	$2.02 \times 10^{-1}s$
FEM-BE	\	$3.69 \times 10^1s$

## 6 Conclusions

This work proposed a model order reduction method for parametric dynamical systems. In the proposed method, time-dependent problems are first transformed into frequency-variable elliptic equations using the Fourier integral transform. The converted equations become time-independent, allowing for parallel computation across different frequency values. To construct an efficient and accurate separable approximation for the resulting complex-valued elliptic equations, we employ the variable-separation-based domain decomposition method. This approach leverages domain decomposition to convert the solution of the complex elliptic problem into solving interface problems and subproblems, making it well-suited for handling complex scenarios. Subsequently, the VS method is applied to establish surrogate models for both the interface problem and the subproblems. Based on this framework, the solution to the time-dependent problem is obtained by applying the inverse Fourier transform to the elliptic equation solutions. A key advantage of the proposed method is its ability to decouple offline and online computations, ensuring that the online phase remains entirely independent of spatial discretization, thus achieving high efficiency. As a result, the overall computational cost of the proposed method is significantly lower than that of standard finite element methods, a fact supported by numerical experiments. Nevertheless, the Fourier transform has inherent limitations, since the functions to be transformed should satisfy certain assumptions. Consequently, this method faces significant constraints when applied to time-dependent problems. In future work, we aim to explore domain decomposition directly on time-dependent problems to achieve efficient computation.

## References

- [1] P. Benner, S. Gugercin and K. Willcox, *A survey of projection-based model reduction methods for parametric dynamical systems*, SIAM Rev., 57, 483-531 (2015).
- [2] S.L. Brunton and J.N. Kutz, *Data-driven science and engineering: machine learning, dynamical systems, and control*, Cambridge University Press (2019).
- [3] T.F. Chan, *Analysis of preconditioners for domain decomposition*, SIAM J. Numer. Anal., 24, 382-390 (1987).
- [4] T.F. Chan and T.P. Mathew, *Domain decomposition algorithms*, Acta Numer., 3, 61-143 (1994).
- [5] L. Chen, Y. Chen, Q. Li and Z. Zhang, *Stochastic domain decomposition based on variable-separation method*, Comput. Methods Appl. Mech. Engrg., 418, 116538 (2024).
- [6] L. Chen, Y. Chen, Q. Li and T. Zhou, *A Dynamical Variable-separation Method for Parameter-dependent Dynamical Systems*, SIAM J. Sci. Comput., 47, A1783-A1808 (2025).
- [7] Y. Chen, J.S. Hesthaven, Y. Maday and J. Rodríguez, *Certified reduced basis methods and output bounds for the harmonic Maxwell's equations*, SIAM J. Sci. Comput., 32, 970-996 (2010).
- [8] Y. Chen, J. Jakeman, C. Gittelsohn and D. Xiu, *Local polynomial chaos expansion for linear differential equations with high dimensional random inputs*, SIAM J. Sci. Comput., 37, A79-A102 (2015).
- [9] J. Douglas, J.E. Santos and D. Sheen, *Approximation of scalar waves in the space-frequency domain*, Math. Models Meth. Appl. Sci., 4, 509-531 (1994).
- [10] J. Douglas, J.E. Santos, D. Sheen and L.S. Bennethum, *Frequency domain treatment of one-dimensional scalar waves*, Math. Model Meth. Appl. Sci., 3, 171-194 (1993).
- [11] M. Drohmann, B. Haasdonk and M. Ohlberger, *Reduced basis approximation for nonlinear parametrized evolution equations based on empirical operator interpolation*, SIAM J. Sci. Comput., 34, A937-A969 (2012).

- [12] M. Esmaily and D. Jia, *A stabilized formulation for the solution of the incompressible unsteady stokes equations in the frequency domain*, J. Comput. Phys., 473, 111736 (2023).
- [13] X. Feng and D. Sheen, *An elliptic regularity estimate for a problem arising from the frequency domain treatment of waves*, Trans. Ams. Math. Soc., 346, 475-487 (1994).
- [14] R. Ghaffari and F. Ghoreishi, *Reduced collocation method for time-dependent parametrized partial differential equations*, Bull. Iran. Math. Soc., 45, 1487-1504 (2019).
- [15] M.A. Grepl and A.T. Patera, *A posteriori error bounds for reduced-basis approximations of parametrized parabolic partial differential equations*, M2AN Math. Model. Numer. Anal., 39, 157-181 (2005).
- [16] M. Guo and J.S. Hesthaven, *Data-driven reduced order modeling for time-dependent problems*, Comput. Methods Appl. Mech. Engrg., 345, 75-99 (2019).
- [17] B. Haasdonk and M. Oehlberger, *Reduced basis method for finite volume approximations of parametrized linear evolution equations*, ESAIM Math. Model. Numer. Anal., 42, 277-302 (2008).
- [18] B. Haasdonk and M. Oehlberger, *Efficient reduced models and a posteriori error estimation for parametrized dynamical systems by offline/online decomposition*, Math. Comput. Model. Dyn. Syst., 17, 145-161 (2011).
- [19] M. Hadigol, A. Doostan, H.G. Matthies and R. Niekamp, *Partitioned treatment of uncertainty in coupled domain problems: A separated representation approach*, Comput. Methods Appl. Mech. Engrg., 274, 103-124 (2014).
- [20] M. Heinkenschloss and H. Nguyen, *Neumann-Neumann domain decomposition preconditioners for linear-quadratic elliptic optimal control problems*, SIAM J. Sci. Comput., 28, 1001-1028 (2006).
- [21] M.W. Hess and P. Benner, *Fast evaluation of time-harmonic Maxwell's equations using the reduced basis method*, IEEE Trans. Microw. Theory Tech., 61, 2265-2274 (2013).
- [22] J.S. Hesthaven, C. Pagliantini and G. Rozza, *Reduced basis methods for time-dependent problems*, Acta Numer., 31, 265-345 (2022).
- [23] J.S. Hesthaven, G. Rozza and B. Stamm, *Certified Reduced Basis Methods for Parametrized Partial Differential Equations*, Springer (2016).
- [24] L. Jiang and Q. Li, *Model reduction method using variable-separation for stochastic saddle point problems*, J. Comput. Phys., 354, 43-66 (2018).
- [25] C.O. Lee, J. Lee and D. Sheen, *Frequency domain formulation of linearized Navier-Stokes equations*, Comput. Methods Appl. Mech. Engrg., 187, 351-362 (2000).
- [26] C.O. Lee, J. Lee, D. Sheen and Y. Yeom, *A frequency-domain parallel method for the numerical approximation of parabolic problems*, Comput. Methods Appl. Mech. Engrg., 169, 19-29 (1999).
- [27] J. Lee and D. Sheen, *An accurate numerical inversion of Laplace transforms based on the location of their poles*, Comput. Math. Appl., 48, 1415-1423 (2004).
- [28] J. Lee and D. Sheen, *A parallel method for backward parabolic problems based on the Laplace transformation*, SIAM J. Numer. Anal., 44, 1466-1486 (2006).
- [29] K. Li, T.Z. Huang, L. Li and S. Lanteri, *Non-intrusive reduced-order modeling of parameterized electromagnetic scattering problems using cubic spline interpolation*, J. Sci. Comput., 87, 1-29 (2021).

- [30] Q. Li and L. Jiang, *A novel variable-separation method based on sparse and low rank representation for stochastic partial differential equations*, SIAM J. Sci. Comput., 39, A2879-A2910 (2017).
- [31] Q. Li and P. Zhang, *A variable-separation method for nonlinear partial differential equations with random inputs*, SIAM J. Sci. Comput., 42, A723-A750 (2020).
- [32] Q. Liao and K. Willcox, *A domain decomposition approach for uncertainty analysis*, SIAM J. Sci. Comput., 37, A103-A133 (2015).
- [33] J. Mandel, *Balancing domain decomposition*, Comm. Numer. Methods Engrg., 9, 233-241 (1993).
- [34] L. Mu and G. Zhang, *A domain decomposition model reduction method for linear convection-diffusion equations with random coefficients*, SIAM J. Sci. Comput., 41, A1984-A2011 (2019).
- [35] A. Nouy and O.P. Le Maître, *Generalized spectral decomposition for stochastic nonlinear problems*, J. Comput. Phys., 228, 202-235 (2009).
- [36] A. Sarkar, N. Benabbou and R. Ghanem, *Domain decomposition of stochastic PDEs: theoretical formulations*, Internat. J. Numer. Methods Engrg., 77, 689-701 (2009).
- [37] T.P. Sapsis and P.F.J. Lermusiaux, *Dynamically orthogonal field equations for continuous stochastic dynamical systems*, Phys. D, 238, 2347-2360 (2009).
- [38] J. Schöberl, *Efficient contact solvers based on domain decomposition techniques*, Comput. Math. Appl., 42, 1217-1228 (2001).
- [39] J.K. Seo and B.C. Shin, *Reduced-order modeling using the frequency-domain method for parabolic partial differential equations*, AIMS Math., 8, 15255-15268 (2023).
- [40] M.K. Sleeman and M. Yano, *Goal-oriented model reduction for parametrized time-dependent nonlinear partial differential equations*, Comput. Methods Appl. Mech. Engrg., 388, 114206 (2022).
- [41] W. Subber and S. Loisel, *Schwarz preconditioners for stochastic elliptic PDEs*, Comput. Methods Appl. Mech. Engrg., 272, 34-57 (2014).
- [42] W. Subber and A. Sarkar, *A domain decomposition method of stochastic PDEs: An iterative solution techniques using a two-level scalable preconditioner*, J. Comput. Phys., 257, 298-317 (2014).